Brains, Arteries, Sea Monsters, and the Future of Astronomy

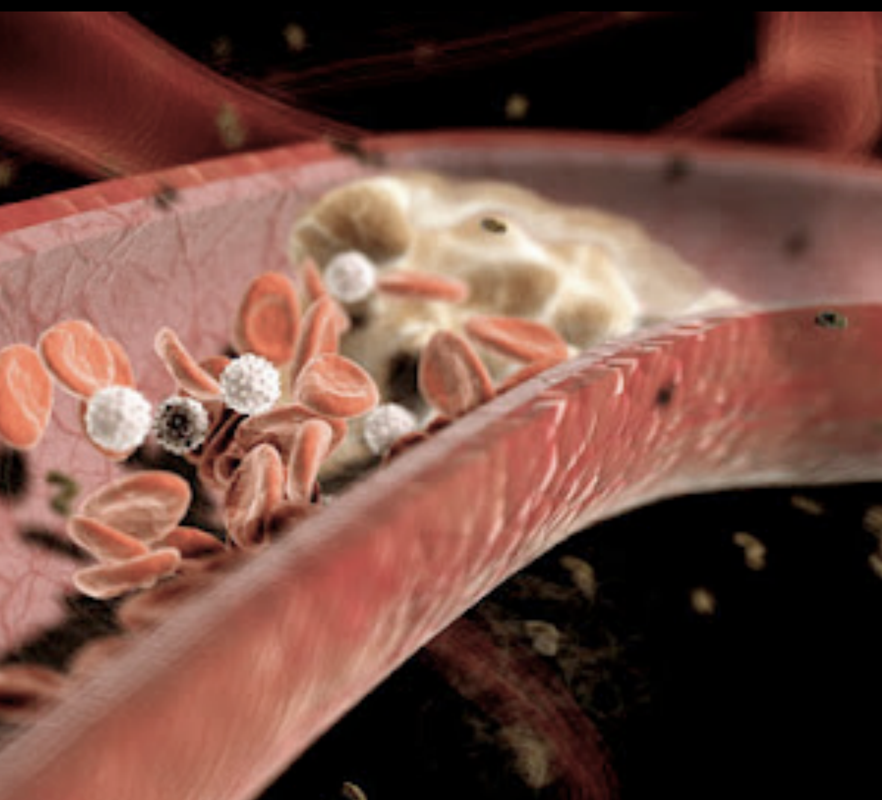

Alyssa A. Goodman
Harvard-Smithsonian Center for Astrophysics

Evolution

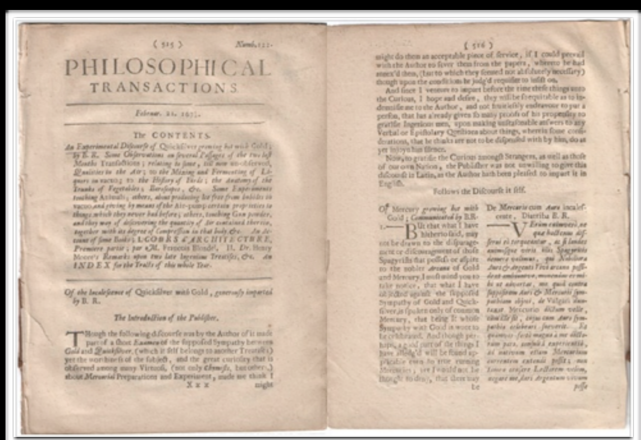

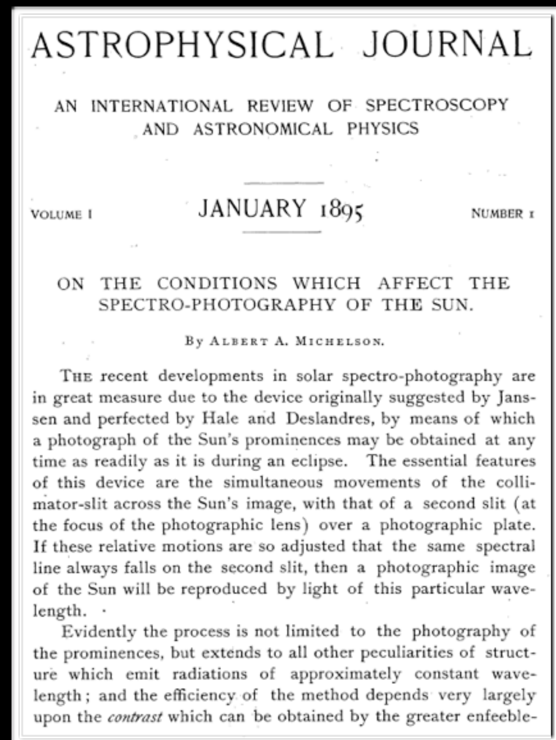

ASTROPHYSICAL JOURNAL

AN INTERNATIONAL REVIEW OF SPECTROSCOPY AND ASTRONOMICAL PHYSICS

VOLUME I — JANUARY 1895 — NUMBER 1

ON THE CONDITIONS WHICH AFFECT THE SPECTRO-PHOTOGRAPHY OF THE SUN.

By ALBERT A. MICHELSON.

THE recent developments in solar spectro-photography are in great measure due to the device originally suggested by Janssen and perfected by Hale and Deslandres, by means of which a photograph of the Sun's prominences may be obtained at any time as readily as it is during an eclipse. The essential features of this device are the simultaneous movements of the collimator-slit across the Sun's image, with that of a second slit (at the focus of the photographic lens) over a photographic plate. If these relative motions are so adjusted that the same spectral line always falls on the second slit, then a photographic image of the Sun will be reproduced by light of this particular wave-length.

Evidently the process is not limited to the photography of the prominences, but extends to all other peculiarities of structure which emit radiations of approximately constant wave-length; and the efficiency of the method depends very largely upon the *contrast* which can be obtained by the greater enfeeble-

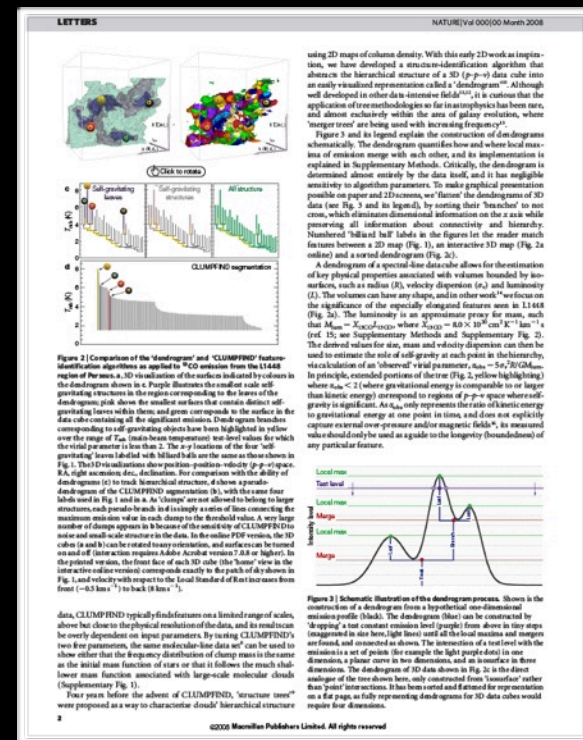

1665 ..230 yr... 1895 ...114 yr... 2009 ...4 yr... 2013

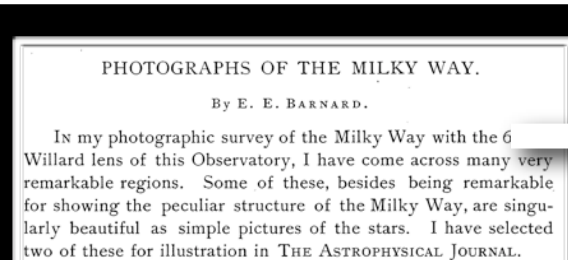

PHOTOGRAPHS OF THE MILKY WAY.

By E. E. BARNARD.

In my photographic survey of the Milky Way with the 6 Willard lens of this Observatory, I have come across many very remarkable regions. Some of these, besides being remarkable for showing the peculiar structure of the Milky Way, are singularly beautiful as simple pictures of the stars. I have selected two of these for illustration in THE ASTROPHYSICAL JOURNAL.

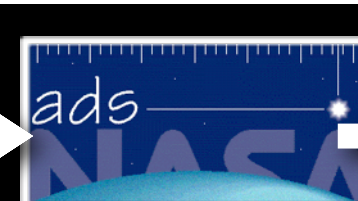

Is the Academic Publishing Industry on the Verge of Disruption?

Brains, Arteries (and star formation)

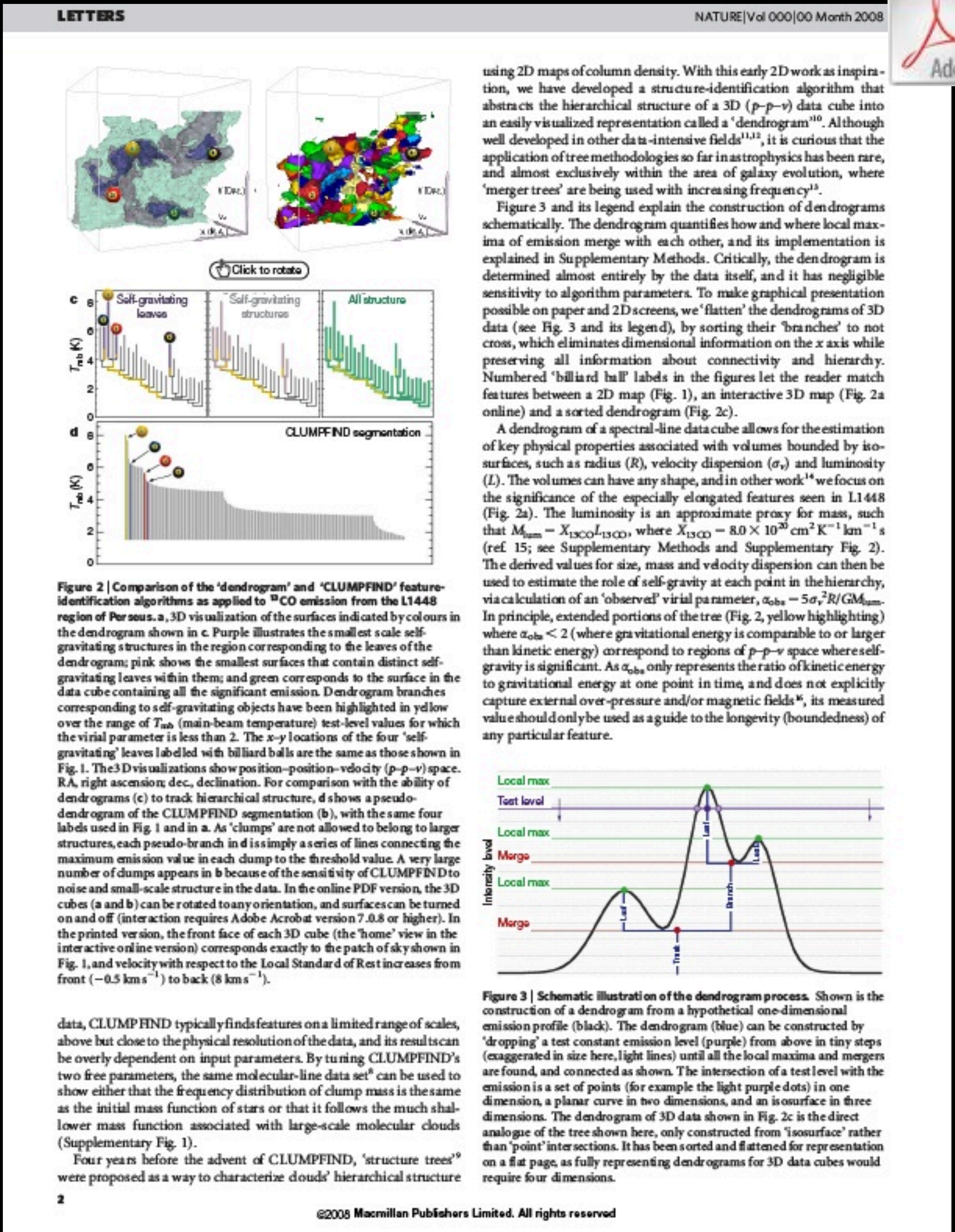

Figure 2 | Comparison of the 'dendrogram' and 'CLUMPFIND' feature-identification algorithms as applied to ^{13}CO emission from the L1448 region of Perseus. a, 3D visualization of the surfaces indicated by colours in the dendrogram shown in c. Purple illustrates the smallest scale self-gravitating structures in the region corresponding to the leaves of the dendrogram; pink shows the smallest surfaces that contain distinct self-gravitating leaves within them; and green corresponds to the surface in the data cube containing all the significant emission. Dendrogram branches corresponding to self-gravitating objects have been highlighted in yellow over the range of T_{mb} (main-beam temperature) test-level values for which the virial parameter is less than 2. The x–y locations of the four 'self-gravitating' leaves labelled with billiard balls are the same as those shown in Fig. 1. The 3D visualizations show position–position–velocity (p–p–v) space. RA, right ascension; dec., declination. For comparison with the ability of dendrograms (c) to track hierarchical structure, d shows a pseudo-dendrogram of the CLUMPFIND segmentation (b), with the same four labels used in Fig. 1 and in a. As 'clumps' are not allowed to belong to larger structures, each pseudo-branch in d is simply a series of lines connecting the maximum emission value in each clump to the threshold value. A very large number of clumps appears in b because of the sensitivity of CLUMPFIND to noise and small-scale structure in the data. In the online PDF version, the 3D cubes (a and b) can be rotated to any orientation, and surfaces can be turned on and off (interaction requires Adobe Acrobat version 7.0.8 or higher). In the printed version, the front face of each 3D cube (the 'home' view in the interactive online version) corresponds exactly to the patch of sky shown in Fig. 1, and velocity with respect to the Local Standard of Rest increases from front ($-0.5\ km\ s^{-1}$) to back ($8\ km\ s^{-1}$).

data, CLUMPFIND typically finds features on a limited range of scales, above but close to the physical resolution of the data, and its results can be overly dependent on input parameters. By tuning CLUMPFIND's two free parameters, the same molecular-line data set[8] can be used to show either that the frequency distribution of clump mass is the same as the initial mass function of stars or that it follows the much shallower mass function associated with large-scale molecular clouds (Supplementary Fig. 1).

Four years before the advent of CLUMPFIND, 'structure trees'[9] were proposed as a way to characterize clouds' hierarchical structure using 2D maps of column density. With this early 2D work as inspiration, we have developed a structure-identification algorithm that abstracts the hierarchical structure of a 3D (p–p–v) data cube into an easily visualized representation called a 'dendrogram'[10]. Although well developed in other data-intensive fields[11,12], it is curious that the application of tree methodologies so far in astrophysics has been rare, and almost exclusively within the area of galaxy evolution, where 'merger trees' are being used with increasing frequency[13].

Figure 3 and its legend explain the construction of dendrograms schematically. The dendrogram quantifies how and where local maxima of emission merge with each other, and its implementation is explained in Supplementary Methods. Critically, the dendrogram is determined almost entirely by the data itself, and it has negligible sensitivity to algorithm parameters. To make graphical presentation possible on paper and 2D screens, we 'flatten' the dendrograms of 3D data (see Fig. 3 and its legend), by sorting their 'branches' to not cross, which eliminates dimensional information on the x axis while preserving all information about connectivity and hierarchy. Numbered 'billiard ball' labels in the figures let the reader match features between a 2D map (Fig. 1), an interactive 3D map (Fig. 2a online) and a sorted dendrogram (Fig. 2c).

A dendrogram of a spectral-line data cube allows for the estimation of key physical properties associated with volumes bounded by isosurfaces, such as radius (R), velocity dispersion (σ_v) and luminosity (L). The volumes can have any shape, and in other work[14] we focus on the significance of the especially elongated features seen in L1448 (Fig. 2a). The luminosity is an approximate proxy for mass, such that $M_{lum} = X_{13CO} L_{13CO}$, where $X_{13CO} = 8.0 \times 10^{20}\ cm^2\ K^{-1}\ km^{-1}\ s$ (ref. 15; see Supplementary Methods and Supplementary Fig. 2). The derived values for size, mass and velocity dispersion can then be used to estimate the role of self-gravity at each point in the hierarchy, via calculation of an 'observed' virial parameter, $\alpha_{obs} = 5\sigma_v^2 R / G M_{lum}$. In principle, extended portions of the tree (Fig. 2, yellow highlighting) where $\alpha_{obs} < 2$ (where gravitational energy is comparable to or larger than kinetic energy) correspond to regions of p–p–v space where self-gravity is significant. As α_{obs} only represents the ratio of kinetic energy to gravitational energy at one point in time, and does not explicitly capture external over-pressure and/or magnetic fields[16], its measured value should only be used as a guide to the longevity (boundedness) of any particular feature.

Figure 3 | Schematic illustration of the dendrogram process. Shown is the construction of a dendrogram from a hypothetical one-dimensional emission profile (black). The dendrogram (blue) can be constructed by 'dropping' a test constant emission level (purple) from above in tiny steps (exaggerated in size here, light lines) until all the local maxima and mergers are found, and connected as shown. The intersection of a test level with the emission is a set of points (for example the light purple dots) in one dimension, a planar curve in two dimensions, and an isosurface in three dimensions. The dendrogram of 3D data shown in Fig. 2c is the direct analogue of the tree shown here, only constructed from 'isosurface' rather than 'point' intersections. It has been sorted and flattened for representation on a flat page, as fully representing dendrograms for 3D data cubes would require four dimensions.

Goodman et al. 2009: 1st 3D PDF in Nature

“Astronomical Medicine”

“KEITH”

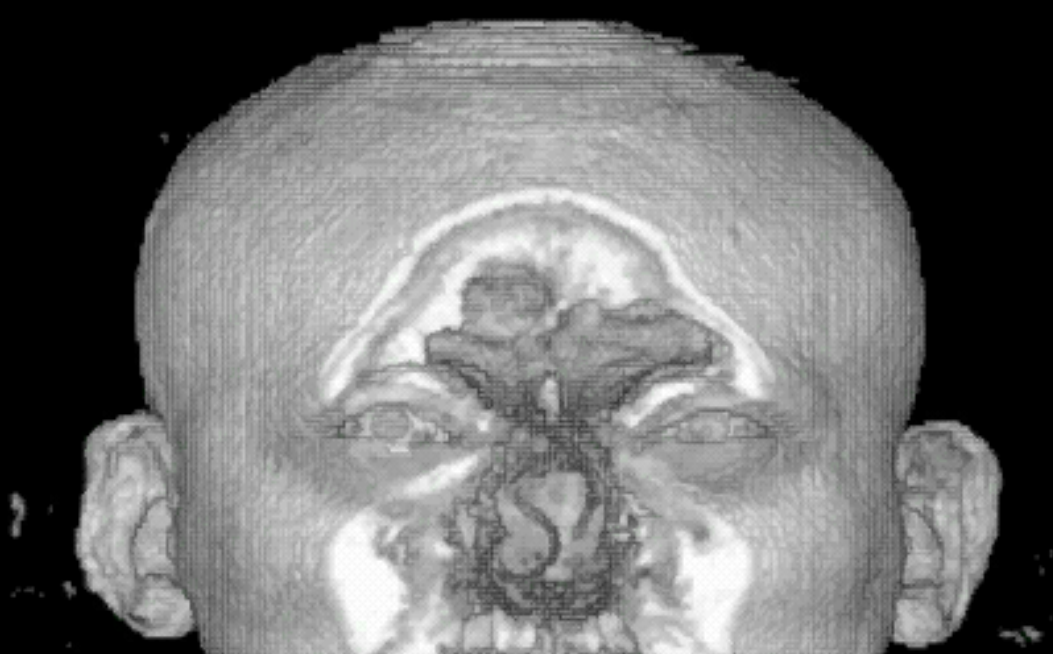

“z” is depth into head

“PERSEUS”

“z” is line-of-sight velocity

http://am.iic.harvard.edu/

High-Dimensional Data: "Cubes"

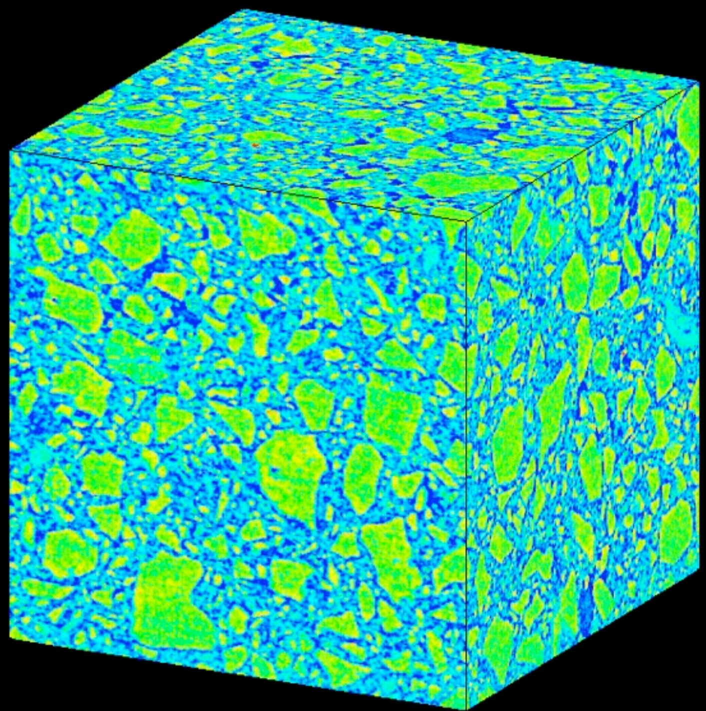

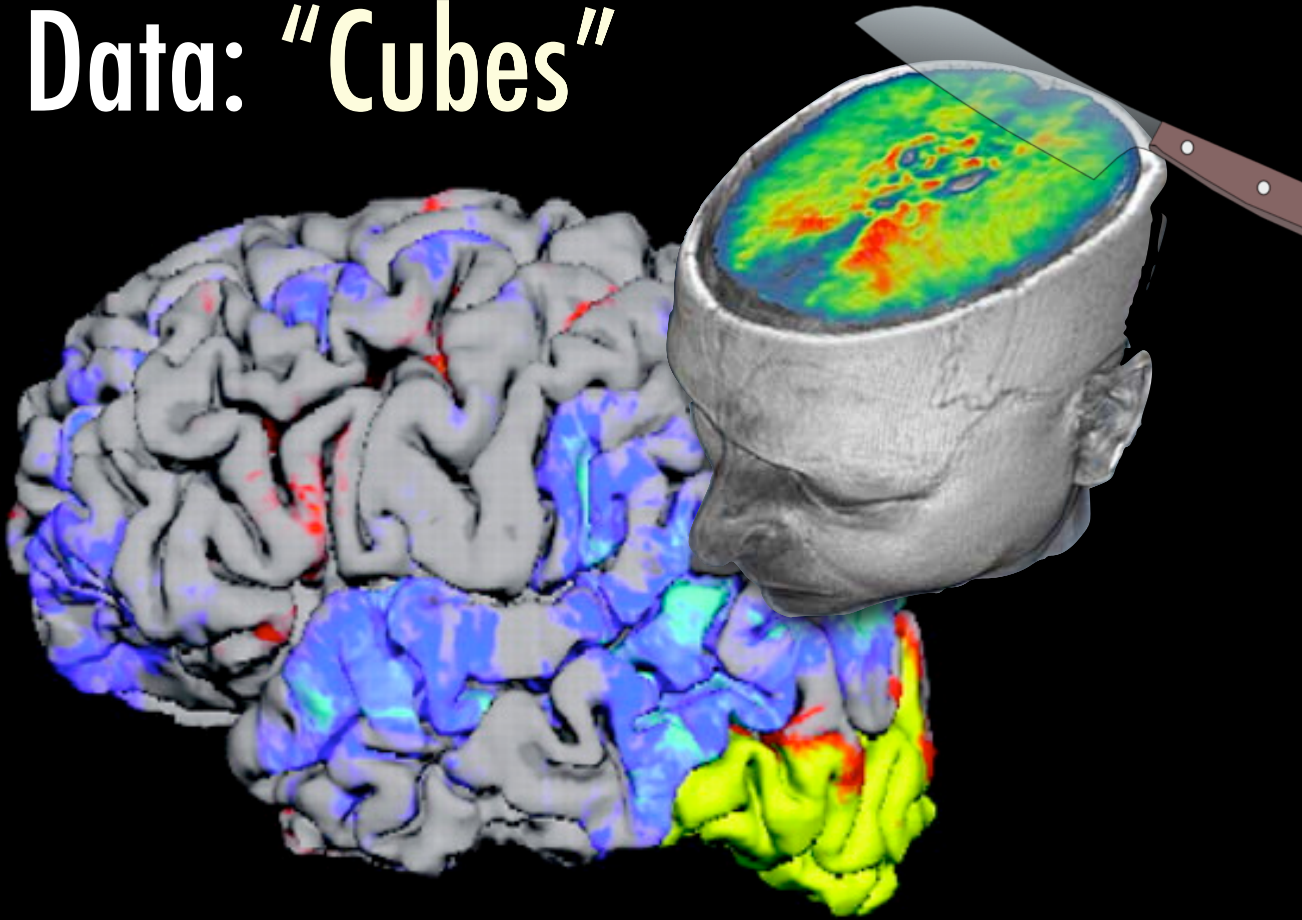

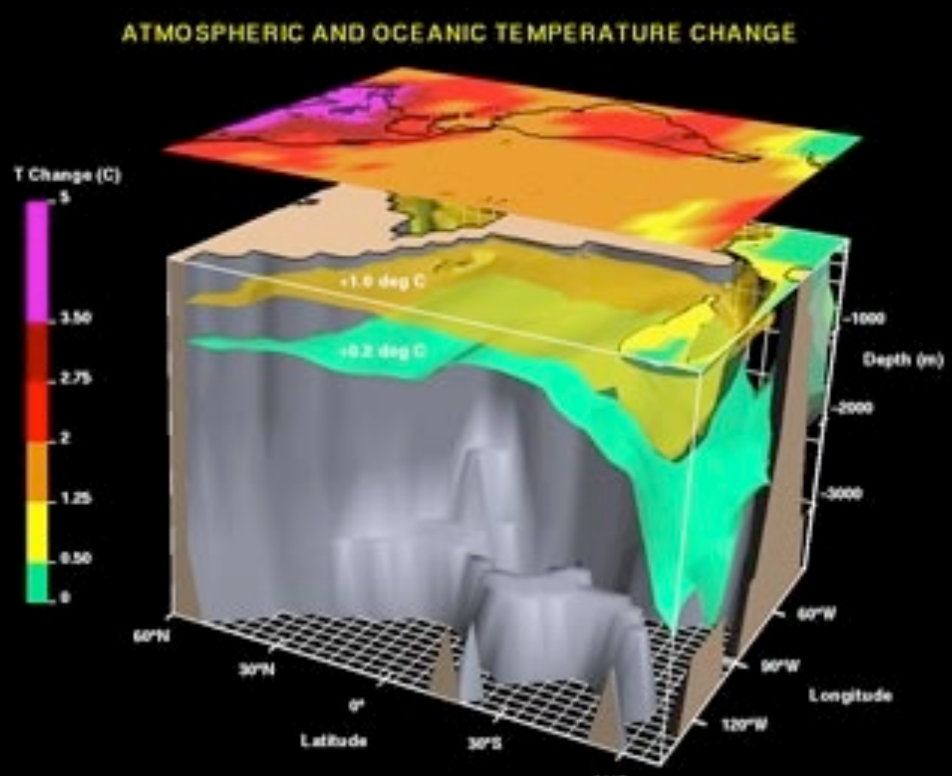

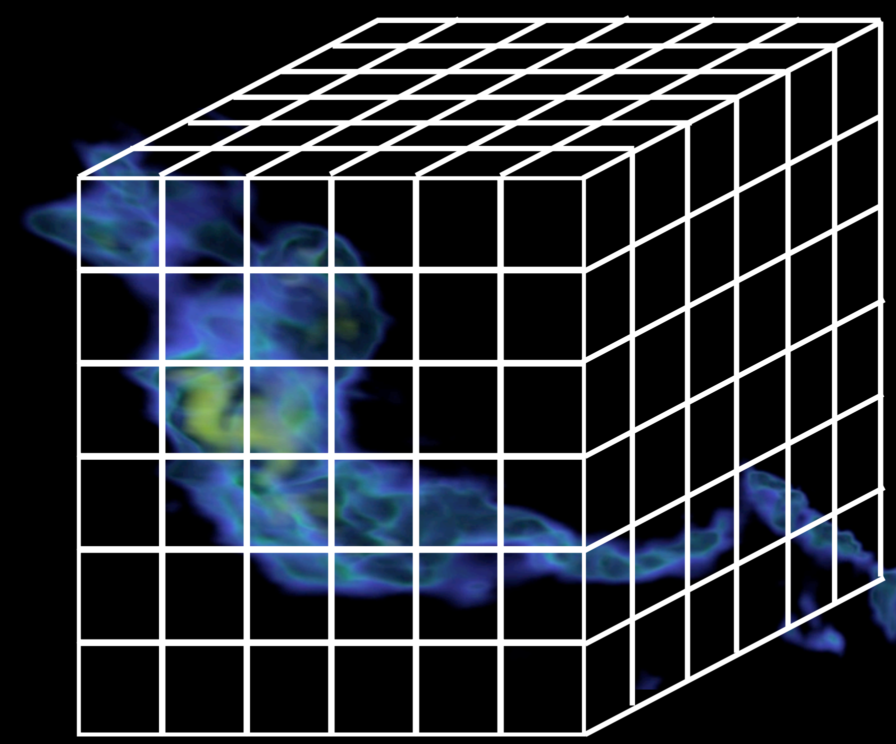

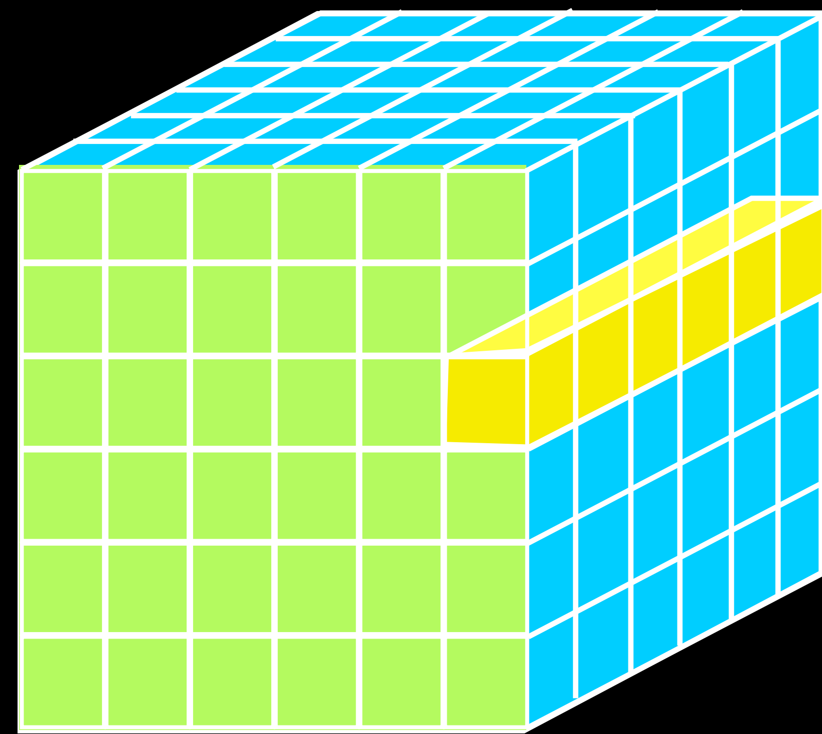

GENERALLY

1D: Columns = "Spectra", "SEDs" or "Time Series"

2D: Faces or Slices = "Images"

3D: Volumes = "3D Renderings", "2D Movies"

4D: Time Series of Volumes = "3D Movies"

Star Formation in Perseus

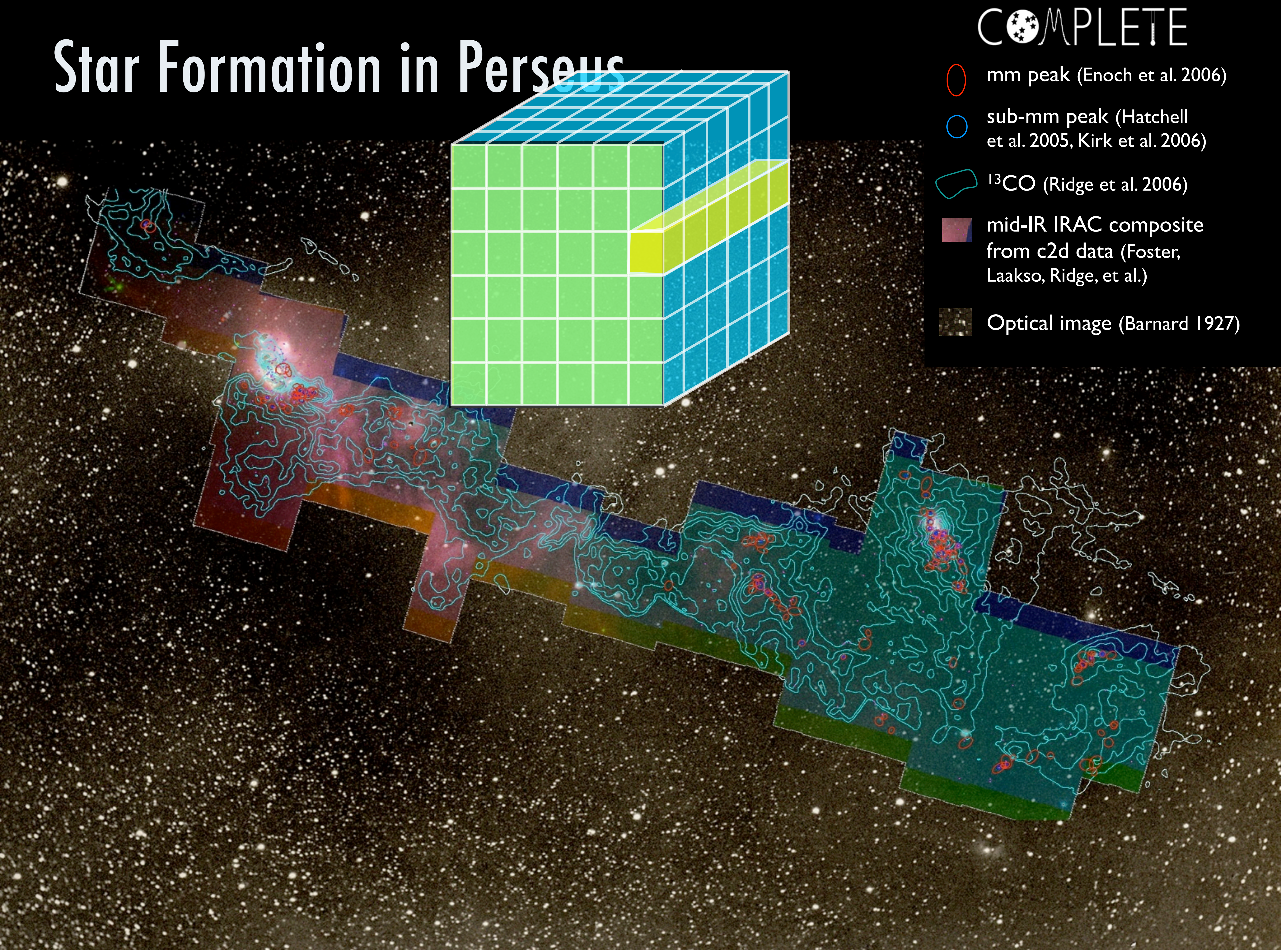

Velocity from Spectroscopy

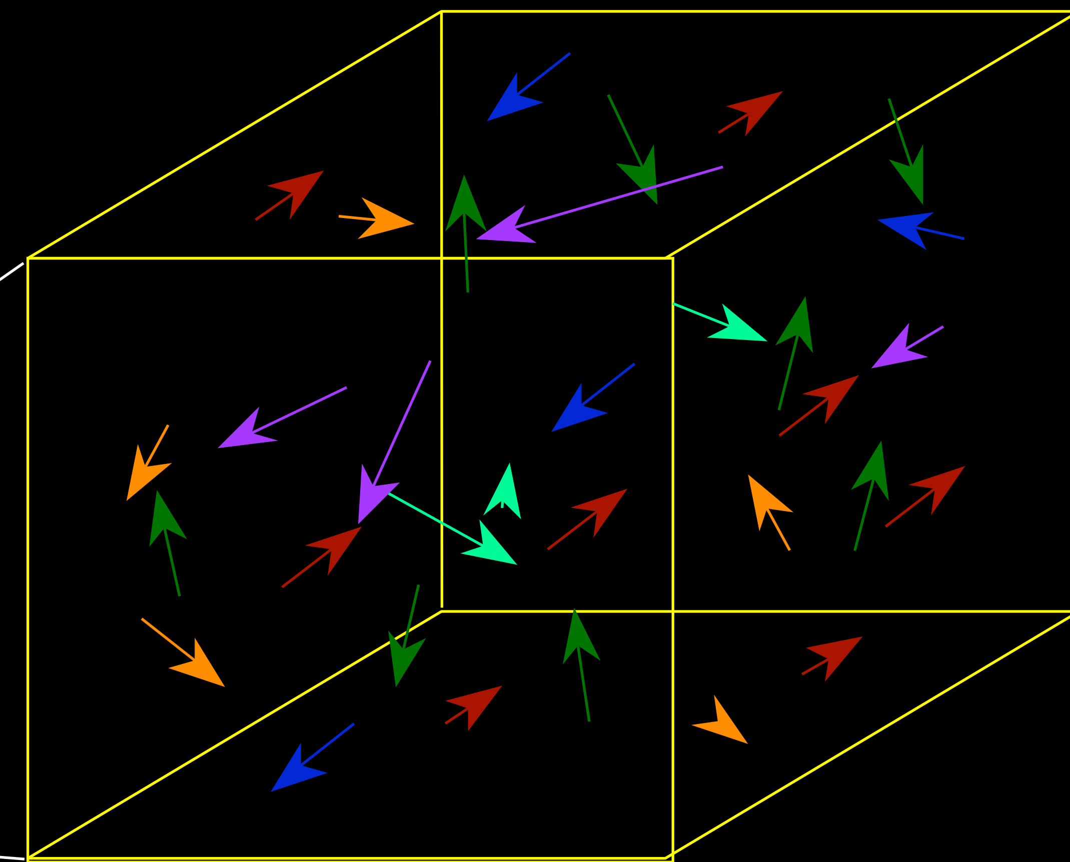

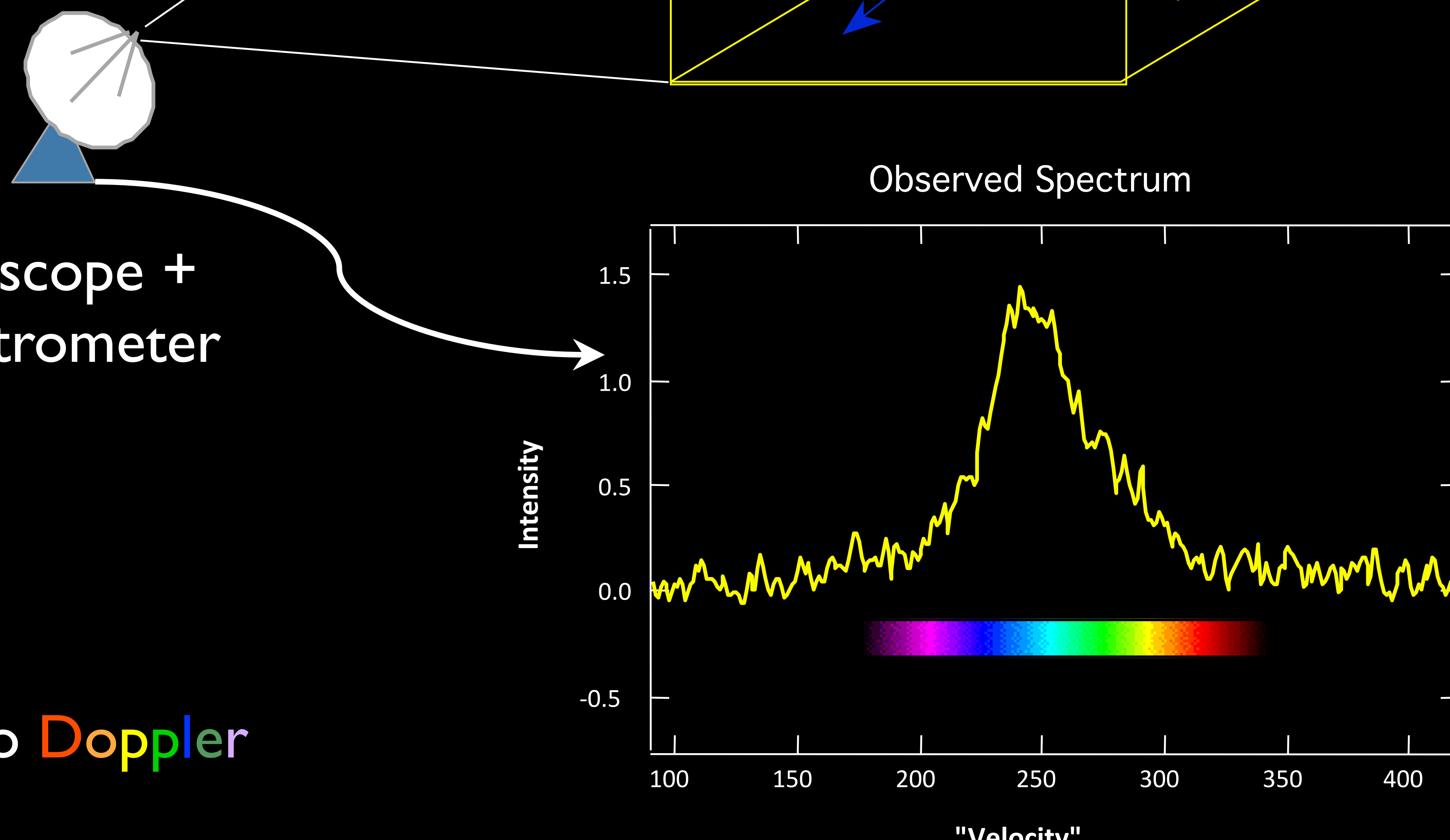

All thanks to Doppler

Spectral-Line Mapping

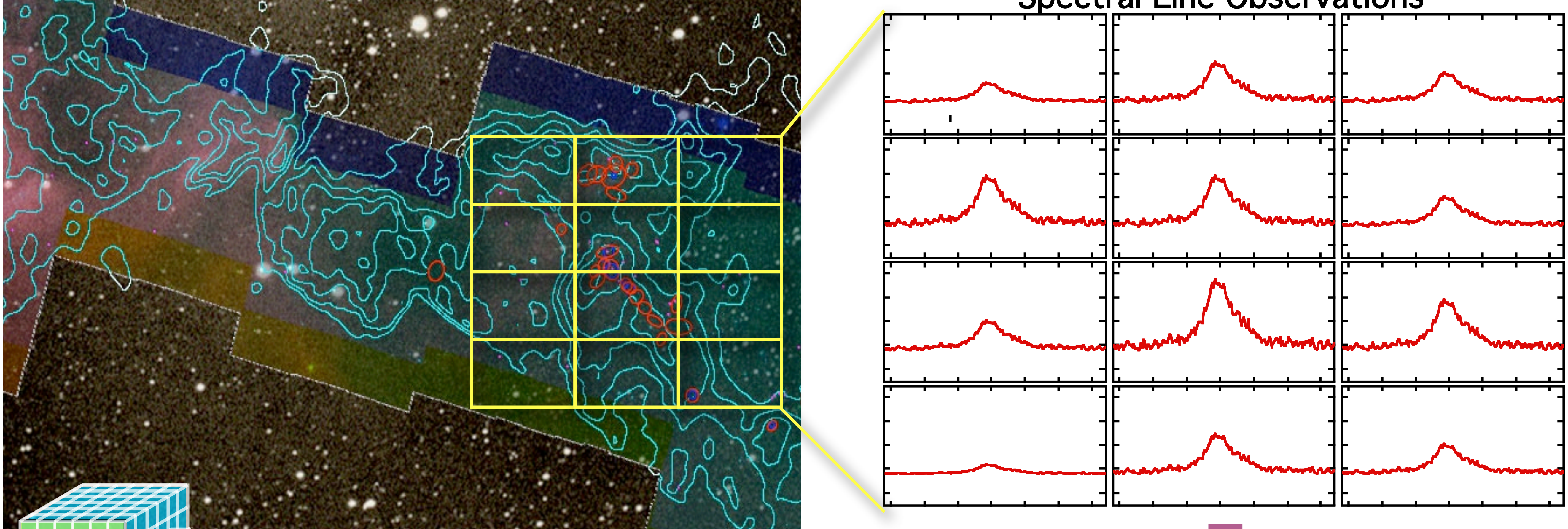

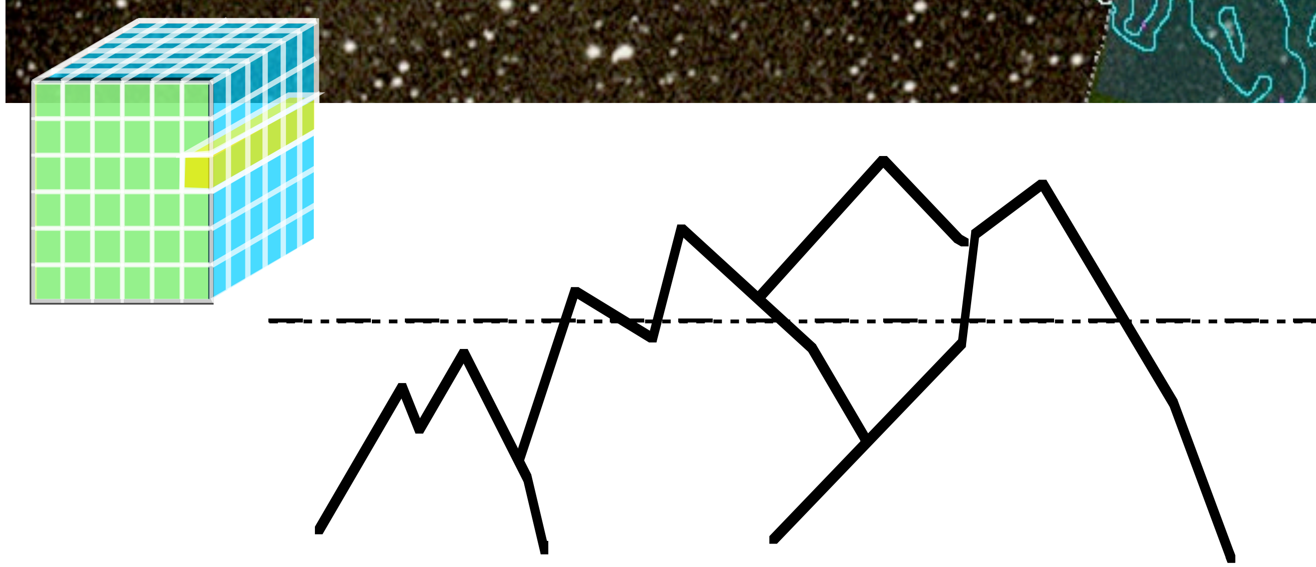

Mountain Range

No loss of information

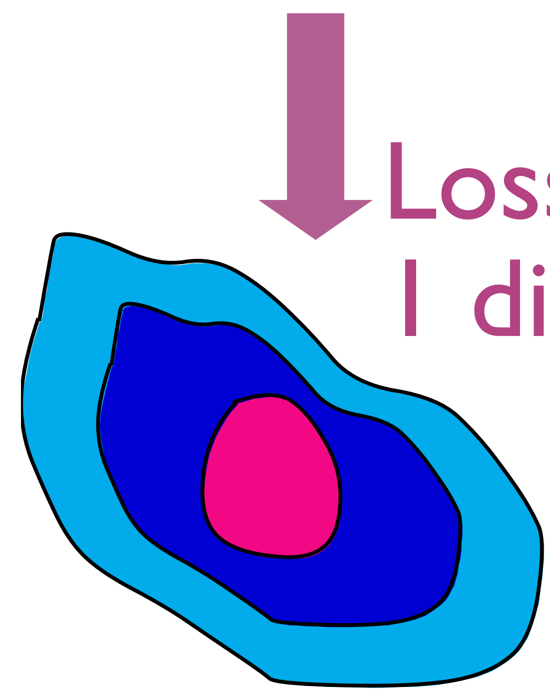

Loss of 1 dimension

COMPLETE Perseus

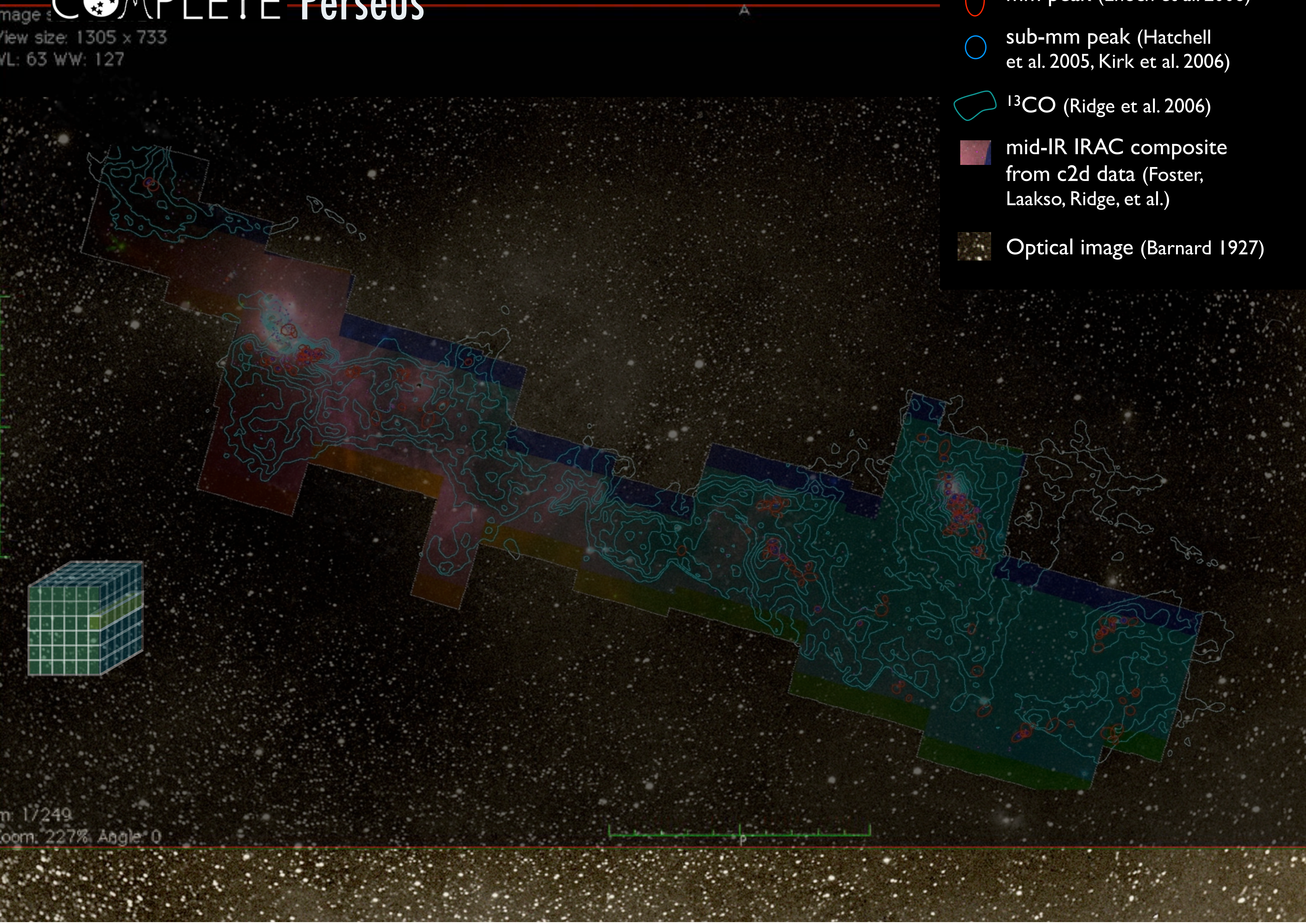

mm peak (Enoch et al. 2006)

sub-mm peak (Hatchell et al. 2005, Kirk et al. 2006)

^{13}CO (Ridge et al. 2006)

mid-IR IRAC composite from c2d data (Foster, Laakso, Ridge, et al.)

Optical image (Barnard 1927)

“Astronomical Medicine”

“KEITH”

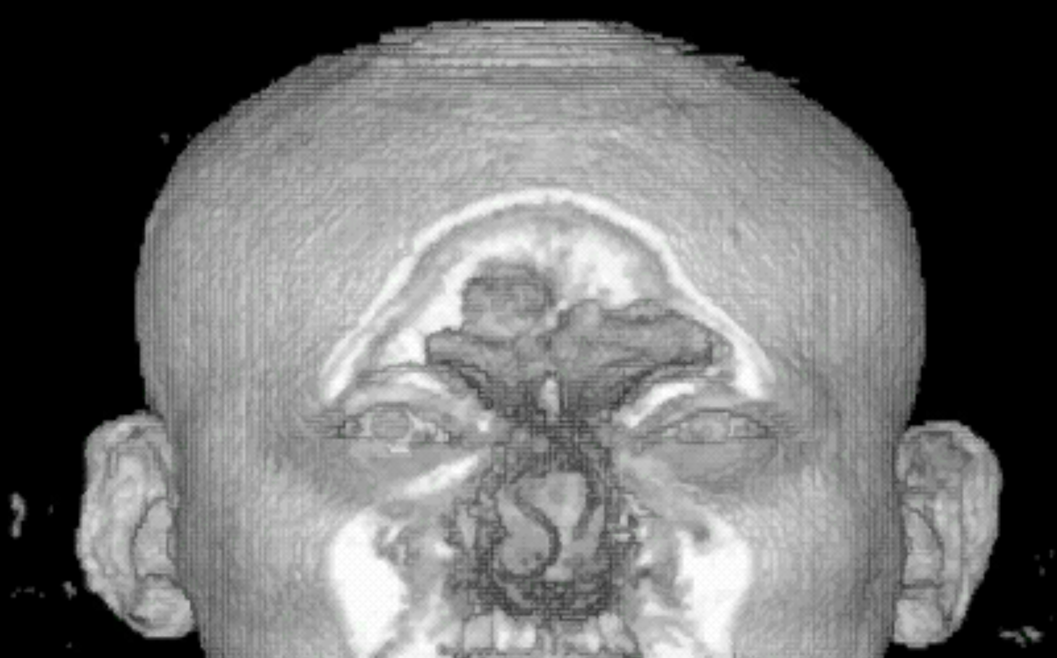

“PERSEUS”

“z” is depth into head

“z” is line-of-sight velocity

http://am.iic.harvard.edu/

COMPLETE Perseus

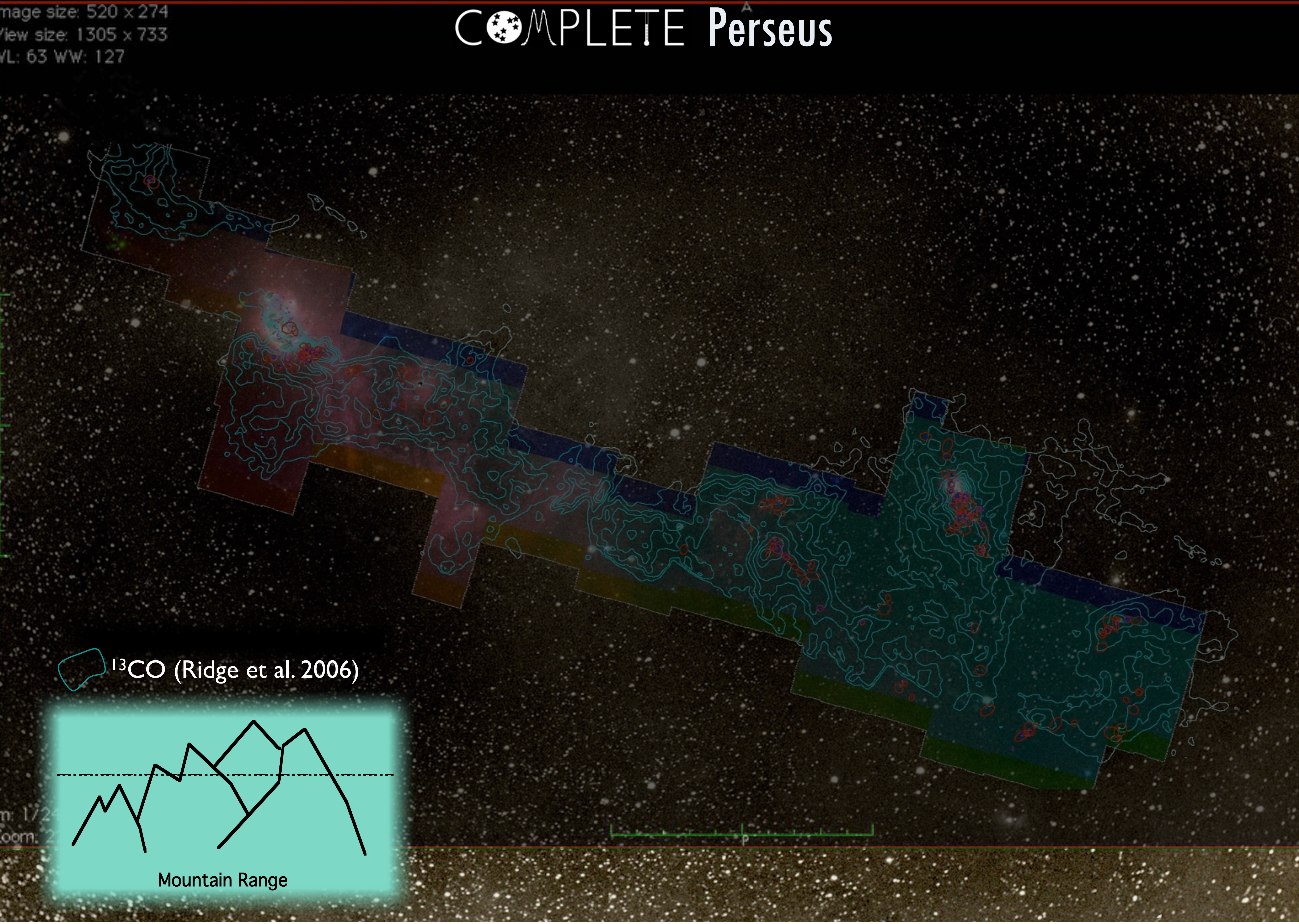

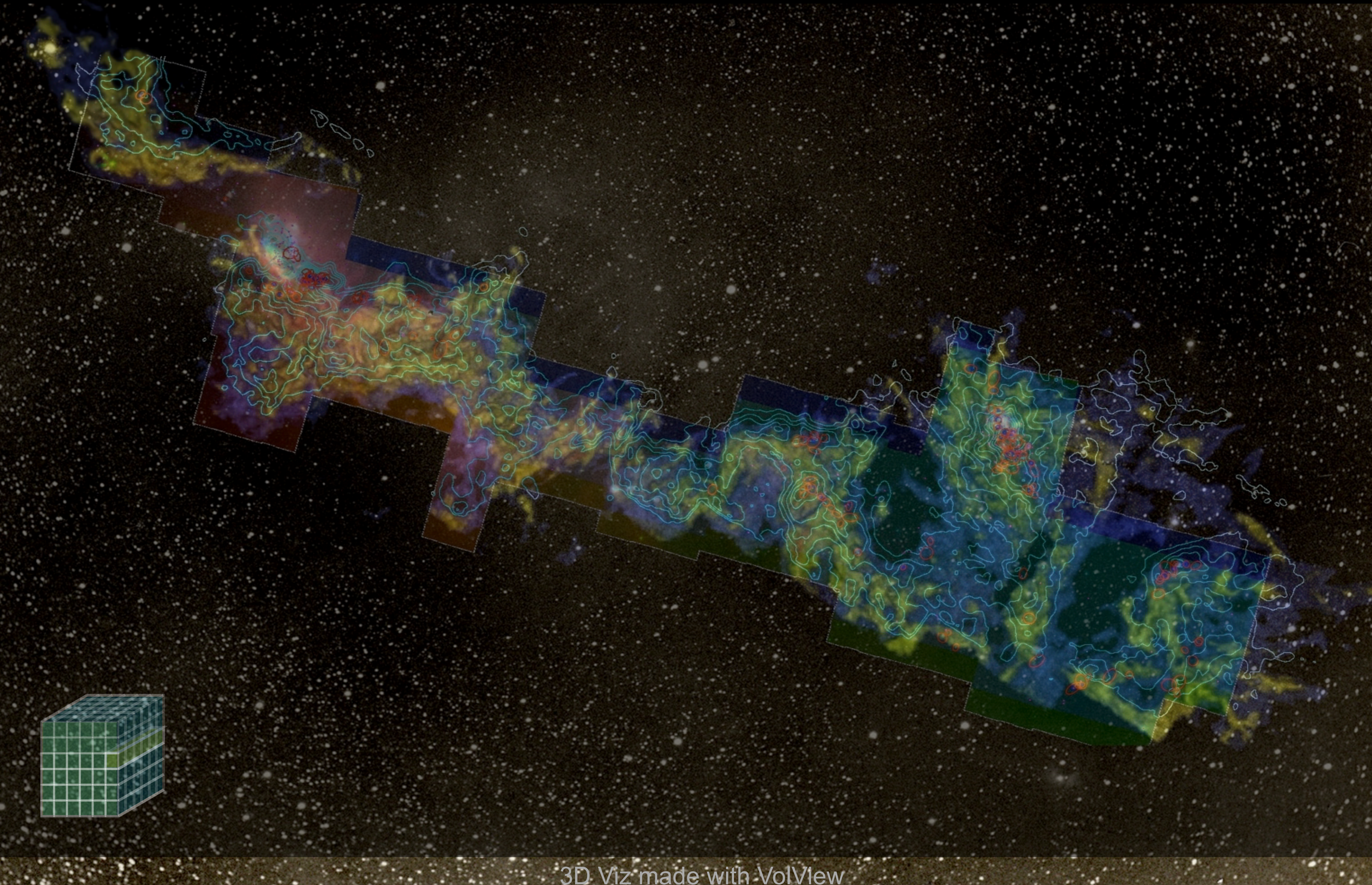

AstronomicalMedicine@IIC

COMPLETE

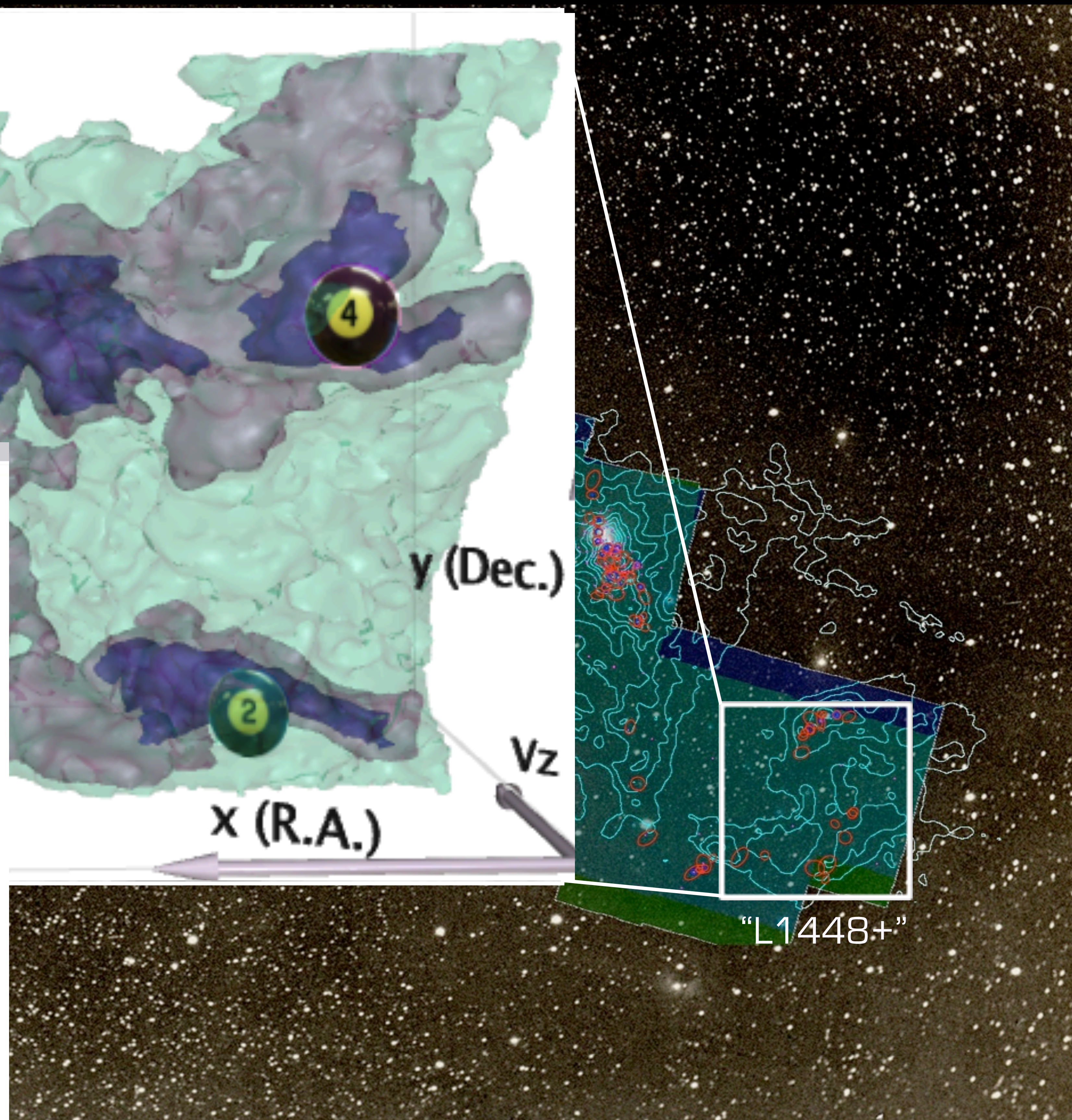

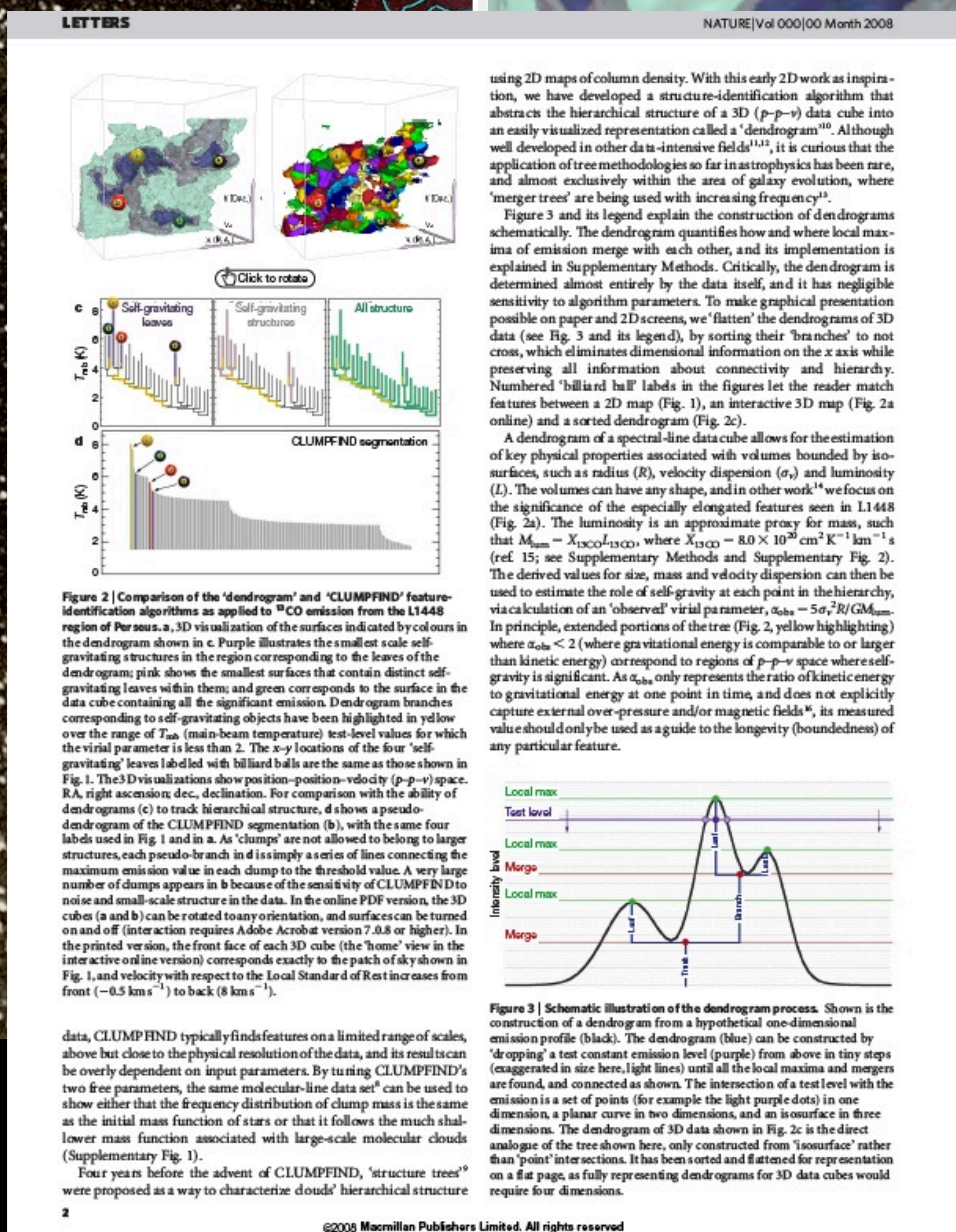

Figure 2 | Comparison of the 'dendrogram' and 'CLUMPFIND' feature-identification algorithms as applied to ^{13}CO emission from the L1448 region of Perseus. **a**, 3D visualization of the surfaces indicated by colours in the dendrogram shown in **c**. Purple illustrates the smallest scale self-gravitating structures in the region corresponding to the leaves of the dendrogram; pink shows the smallest surfaces that contain distinct self-gravitating leaves within them; and green corresponds to the surface in the data cube containing all the significant emission. Dendrogram branches corresponding to self-gravitating objects have been highlighted in yellow over the range of T_{mb} (main-beam temperature) test-level values for which the virial parameter is less than 2. The *x*–*y* locations of the four 'self-gravitating' leaves labelled with billiard balls are the same as those shown in Fig. 1. The 3D visualizations show position–position–velocity (*p*–*p*–*v*) space. RA, right ascension; dec., declination. For comparison with the ability of dendrograms (**c**) to track hierarchical structure, **d** shows a pseudo-dendrogram of the CLUMPFIND segmentation (**b**), with the same four labels used in Fig. 1 and in **a**. As 'clumps' are not allowed to belong to larger structures, each pseudo-branch in **d** is simply a series of lines connecting the maximum emission value in each clump to the threshold value. A very large number of clumps appears in **b** because of the sensitivity of CLUMPFIND to noise and small-scale structure in the data. In the online PDF version, the 3D cubes (**a** and **b**) can be rotated to any orientation, and surfaces can be turned on and off (interaction requires Adobe Acrobat version 7.0.8 or higher). In the printed version, the front face of each 3D cube (the 'home' view in the interactive online version) corresponds exactly to the patch of sky shown in Fig. 1, and velocity with respect to the Local Standard of Rest increases from front (-0.5 km s^{-1}) to back (8 km s^{-1}).

data, CLUMPFIND typically finds features on a limited range of scales, above but close to the physical resolution of the data, and its results can be overly dependent on input parameters. By tuning CLUMPFIND's two free parameters, the same molecular-line data set[8] can be used to show either that the frequency distribution of clump mass is the same as the initial mass function of stars or that it follows the much shallower mass function associated with large-scale molecular clouds (Supplementary Fig. 1).

Four years before the advent of CLUMPFIND, 'structure trees'[9] were proposed as a way to characterize clouds' hierarchical structure using 2D maps of column density. With this early 2D work as inspiration, we have developed a structure-identification algorithm that abstracts the hierarchical structure of a 3D (*p*–*p*–*v*) data cube into an easily visualized representation called a 'dendrogram'[10]. Although well developed in other data-intensive fields[11,12], it is curious that the application of tree methodologies so far in astrophysics has been rare, and almost exclusively within the area of galaxy evolution, where 'merger trees' are being used with increasing frequency[13].

Figure 3 and its legend explain the construction of dendrograms schematically. The dendrogram quantifies how and where local maxima of emission merge with each other, and its implementation is explained in Supplementary Methods. Critically, the dendrogram is determined almost entirely by the data itself, and it has negligible sensitivity to algorithm parameters. To make graphical presentation possible on paper and 2D screens, we 'flatten' the dendrograms of 3D data (see Fig. 3 and its legend), by sorting their 'branches' to not cross, which eliminates dimensional information on the *x* axis while preserving all information about connectivity and hierarchy. Numbered 'billiard ball' labels in the figures let the reader match features between a 2D map (Fig. 1), an interactive 3D map (Fig. 2a online) and a sorted dendrogram (Fig. 2c).

A dendrogram of a spectral-line data cube allows for the estimation of key physical properties associated with volumes bounded by isosurfaces, such as radius (R), velocity dispersion (σ_v) and luminosity (L). The volumes can have any shape, and in other work[14] we focus on the significance of the especially elongated features seen in L1448 (Fig. 2a). The luminosity is an approximate proxy for mass, such that $M_{lum} = X_{13CO}L_{13CO}$, where $X_{13CO} = 8.0 \times 10^{20}$ cm^2 K^{-1} km^{-1} s (ref. 15; see Supplementary Methods and Supplementary Fig. 2). The derived values for size, mass and velocity dispersion can then be used to estimate the role of self-gravity at each point in the hierarchy, via calculation of an 'observed' virial parameter, $\alpha_{obs} = 5\sigma_v^2 R/GM_{lum}$. In principle, extended portions of the tree (Fig. 2, yellow highlighting) where $\alpha_{obs} < 2$ (where gravitational energy is comparable to or larger than kinetic energy) correspond to regions of *p*–*p*–*v* space where self-gravity is significant. As α_{obs} only represents the ratio of kinetic energy to gravitational energy at one point in time, and does not explicitly capture external over-pressure and/or magnetic fields[16], its measured value should only be used as a guide to the longevity (boundedness) of any particular feature.

Figure 3 | Schematic illustration of the dendrogram process. Shown is the construction of a dendrogram from a hypothetical one-dimensional emission profile (black). The dendrogram (blue) can be constructed by 'dropping' a test constant emission level (purple) from above in tiny steps (exaggerated in size here, light lines) until all the local maxima and mergers are found, and connected as shown. The intersection of a test level with the emission is a set of points (for example the light purple dots) in one dimension, a planar curve in two dimensions, and an isosurface in three dimensions. The dendrogram of 3D data shown in Fig. 2c is the direct analogue of the tree shown here, only constructed from 'isosurface' rather than 'point' intersections. It has been sorted and flattened for representation on a flat page, as fully representing dendrograms for 3D data cubes would require four dimensions.

COMPLETE

Arteries

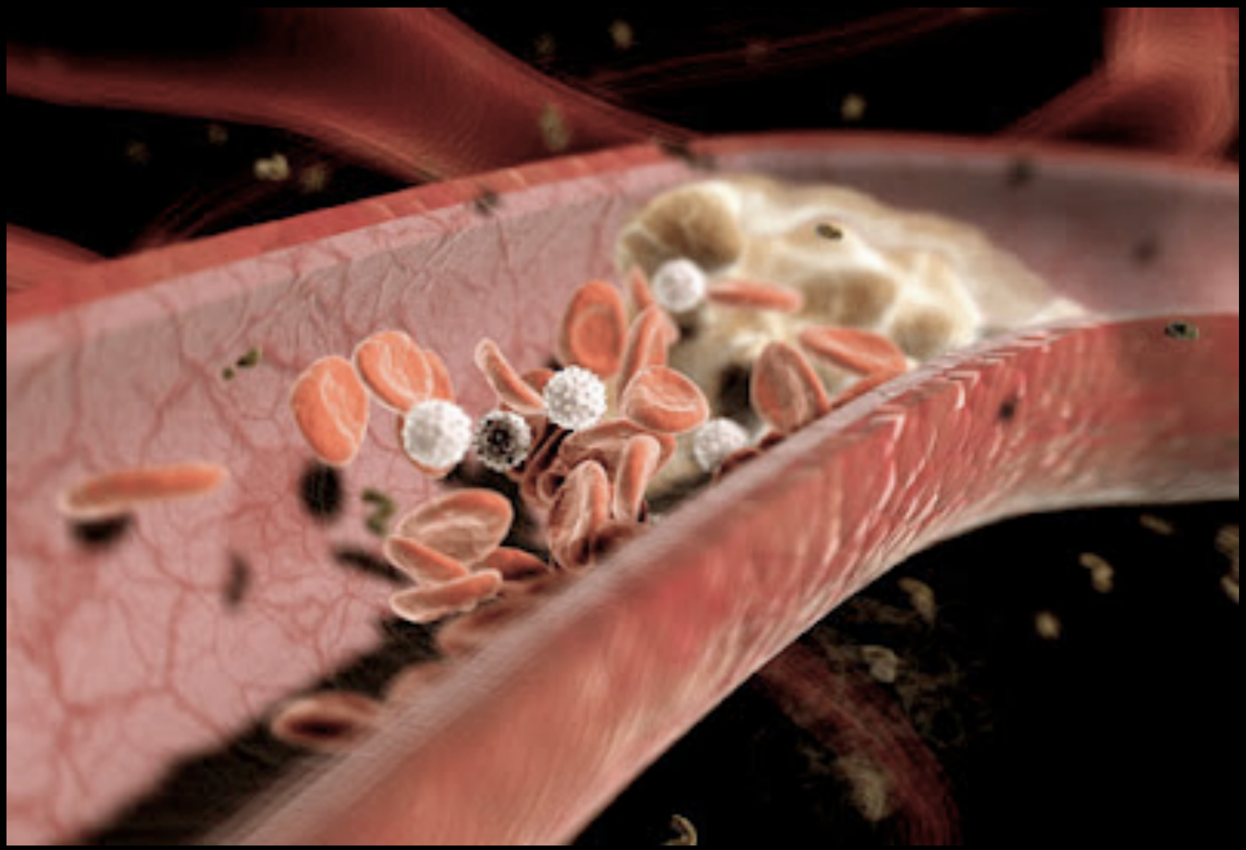

Michelle Borkin

Harvard School of Engineering & Applied Science Ph.D. student,
supervised by Alyssa Goodman (Astronomer) & Hanspeter Pfister (Computer Scientist)

Patients Troubled Hearts, in 3D

Obtain patient CT data

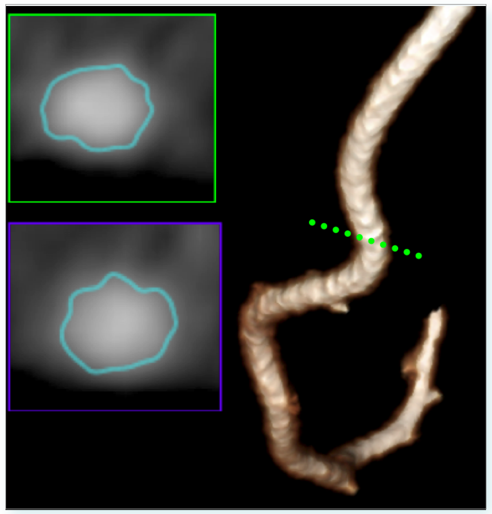

Segment arteries

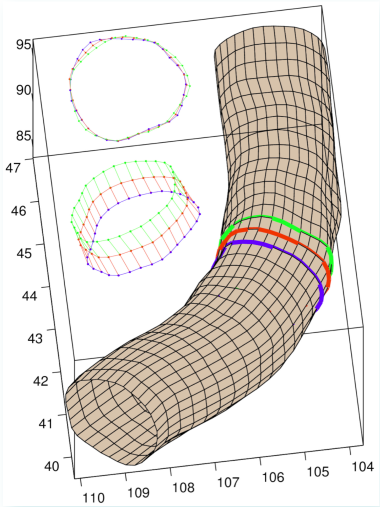

Generate patient geometries

Patient specific flow simulation

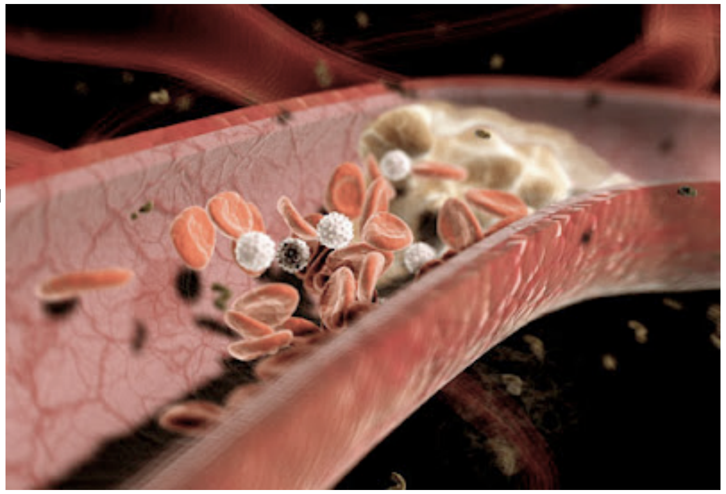

Visualize/analyze data

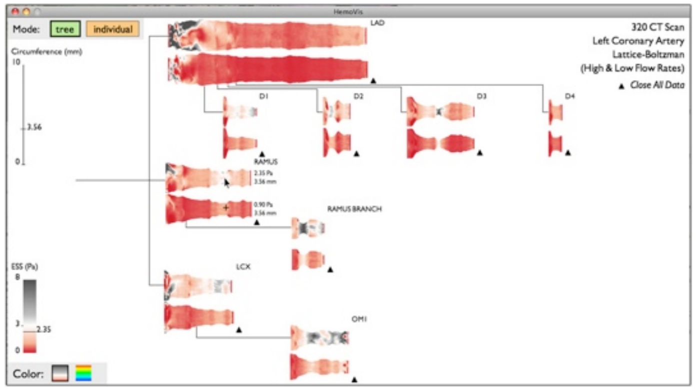

Clinical decision

How much does viz matter?

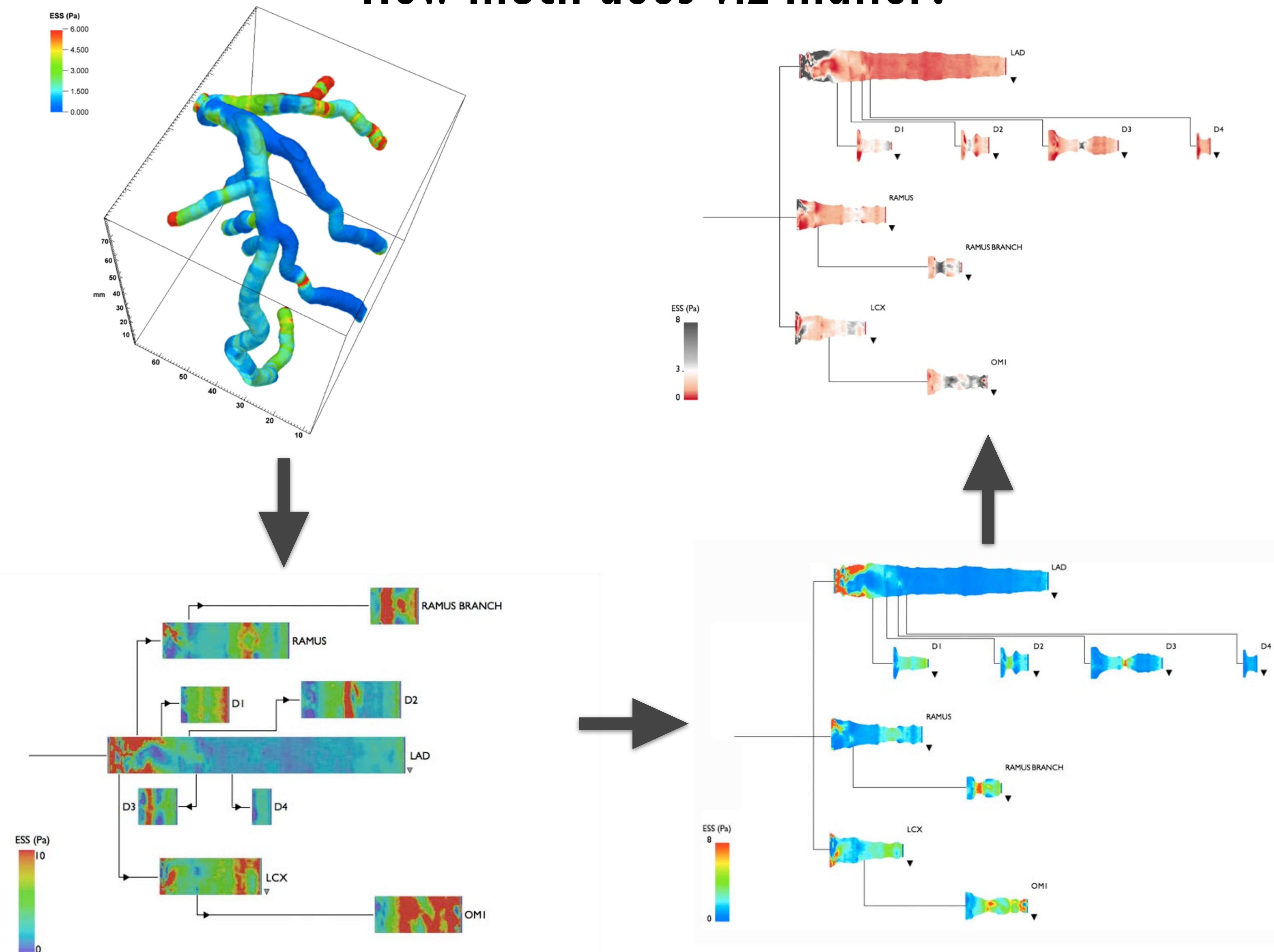

Borkin et al. 2011

ACCURACY

Strong effect of **dimensionality** on accuracy

And strong effect of **color**...

39% *percent low ESS regions found* 62%

91%

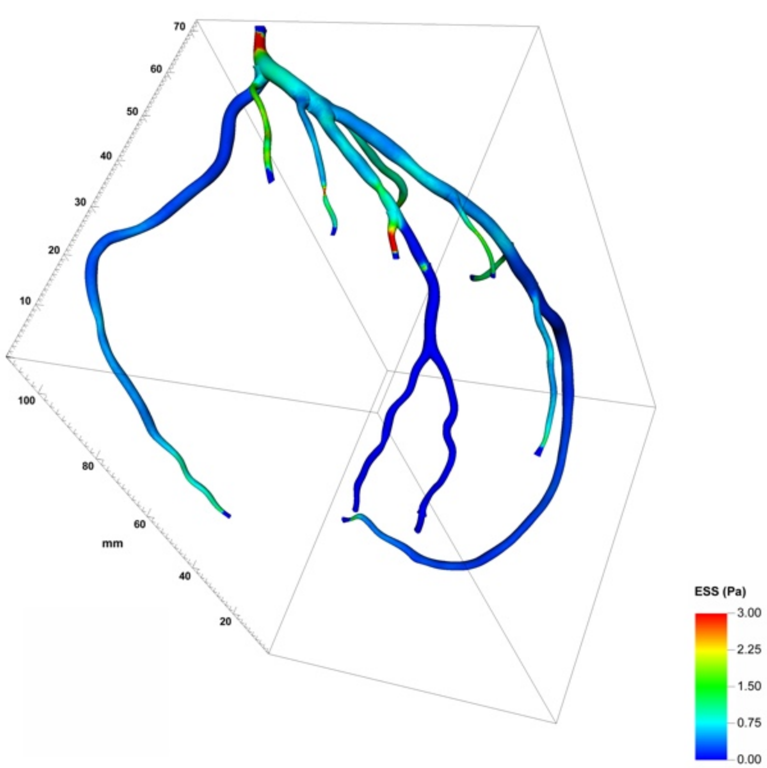

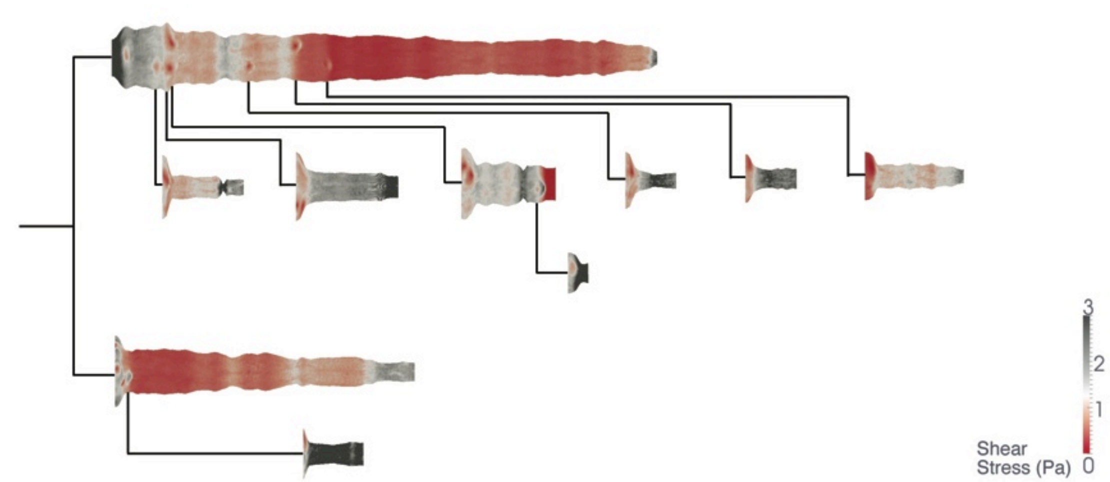

Borkin et al. 2011

EFFICIENCY

Participants more **efficient** in **2D**.

Rainbow color map has greater detriment in 3D.

10.2 sec/region
5.6 sec/region

2.6 sec/region
2.4 sec/region

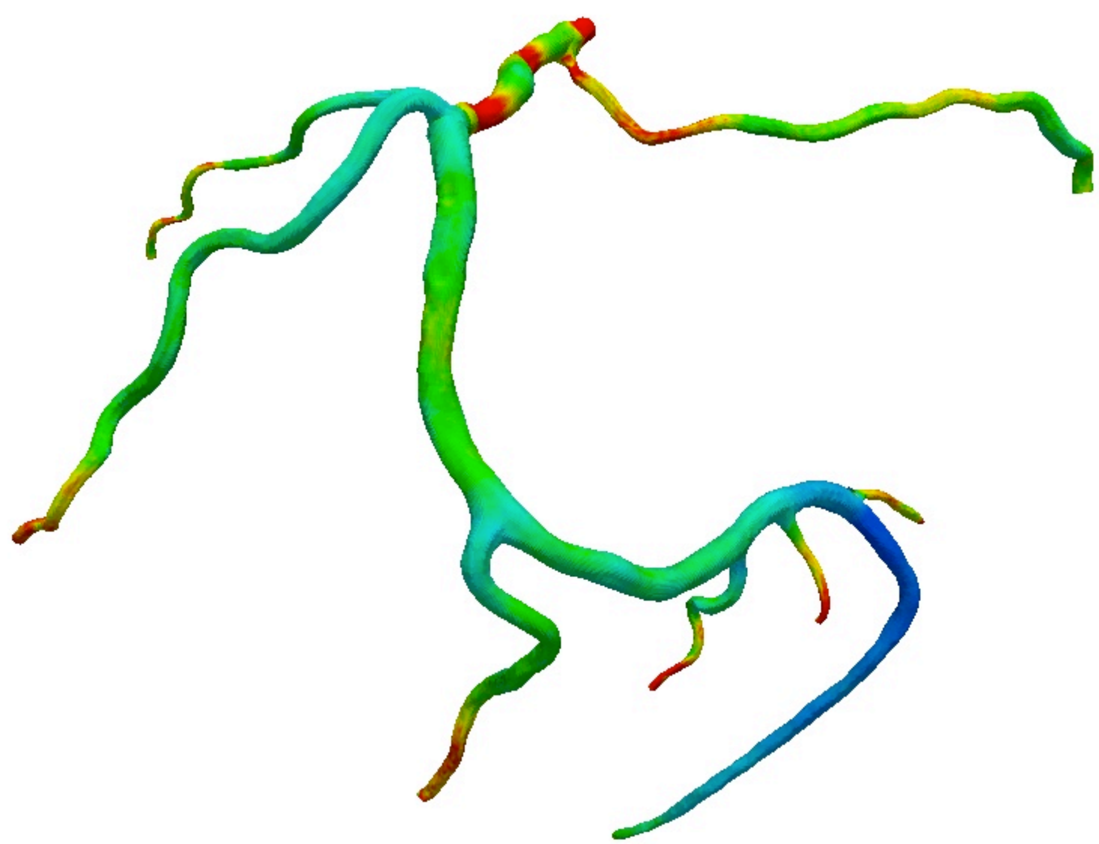

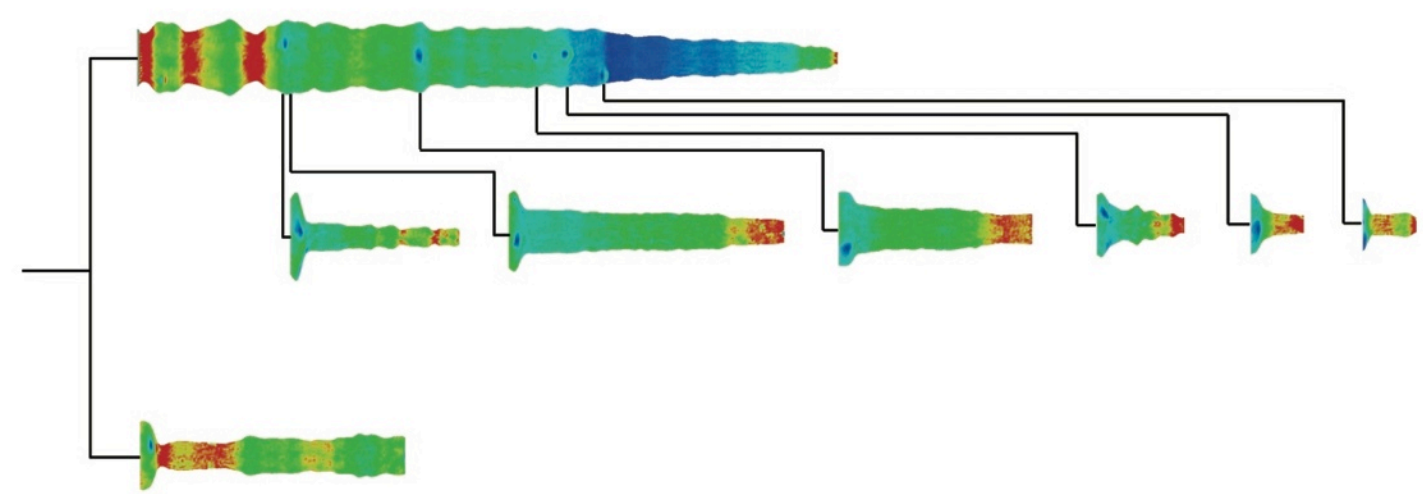

BUT–3D still essential for sugical planning.

Borkin et al. 2011

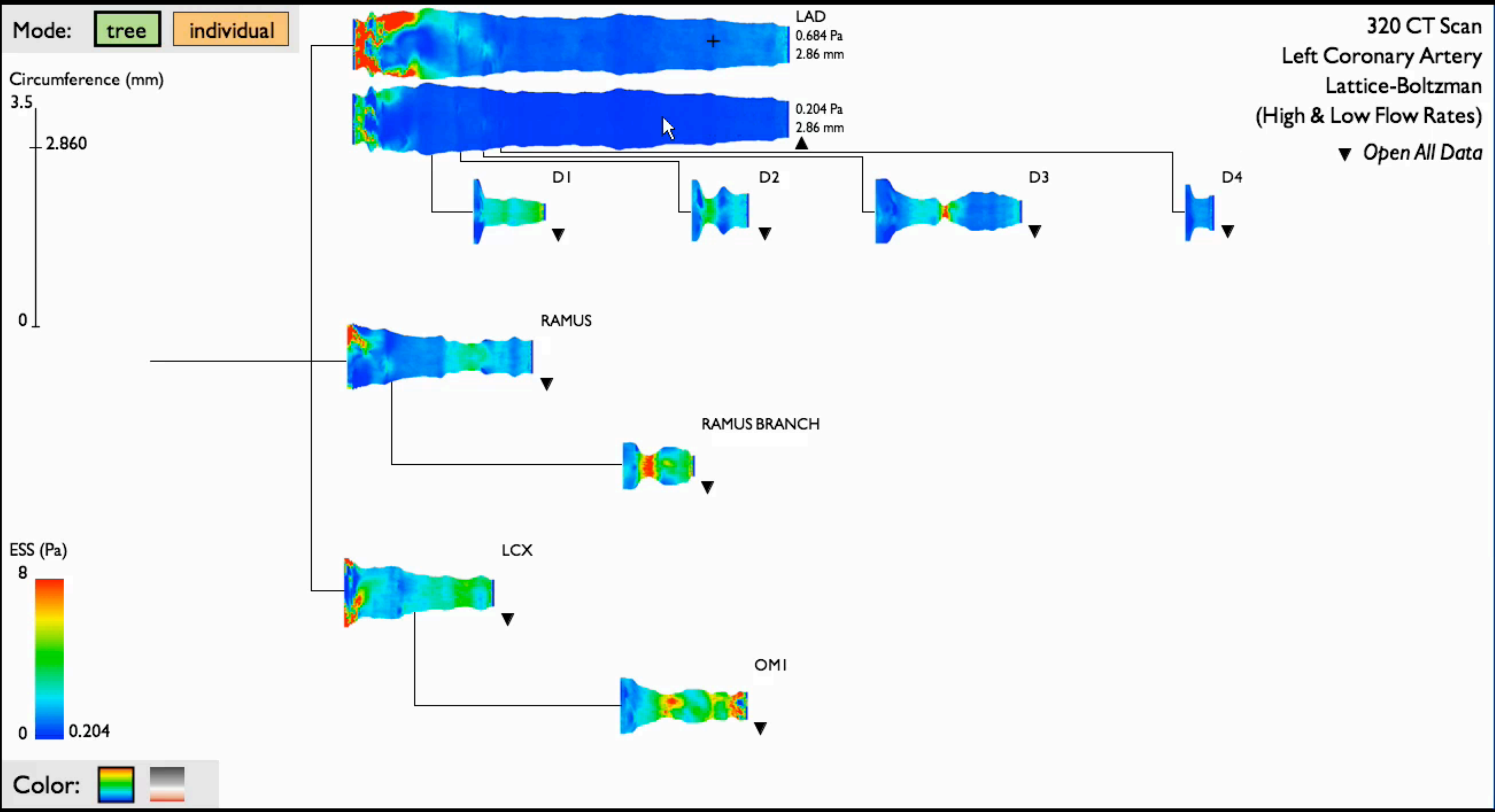

Borkin et al. 2011

“Linked Views”

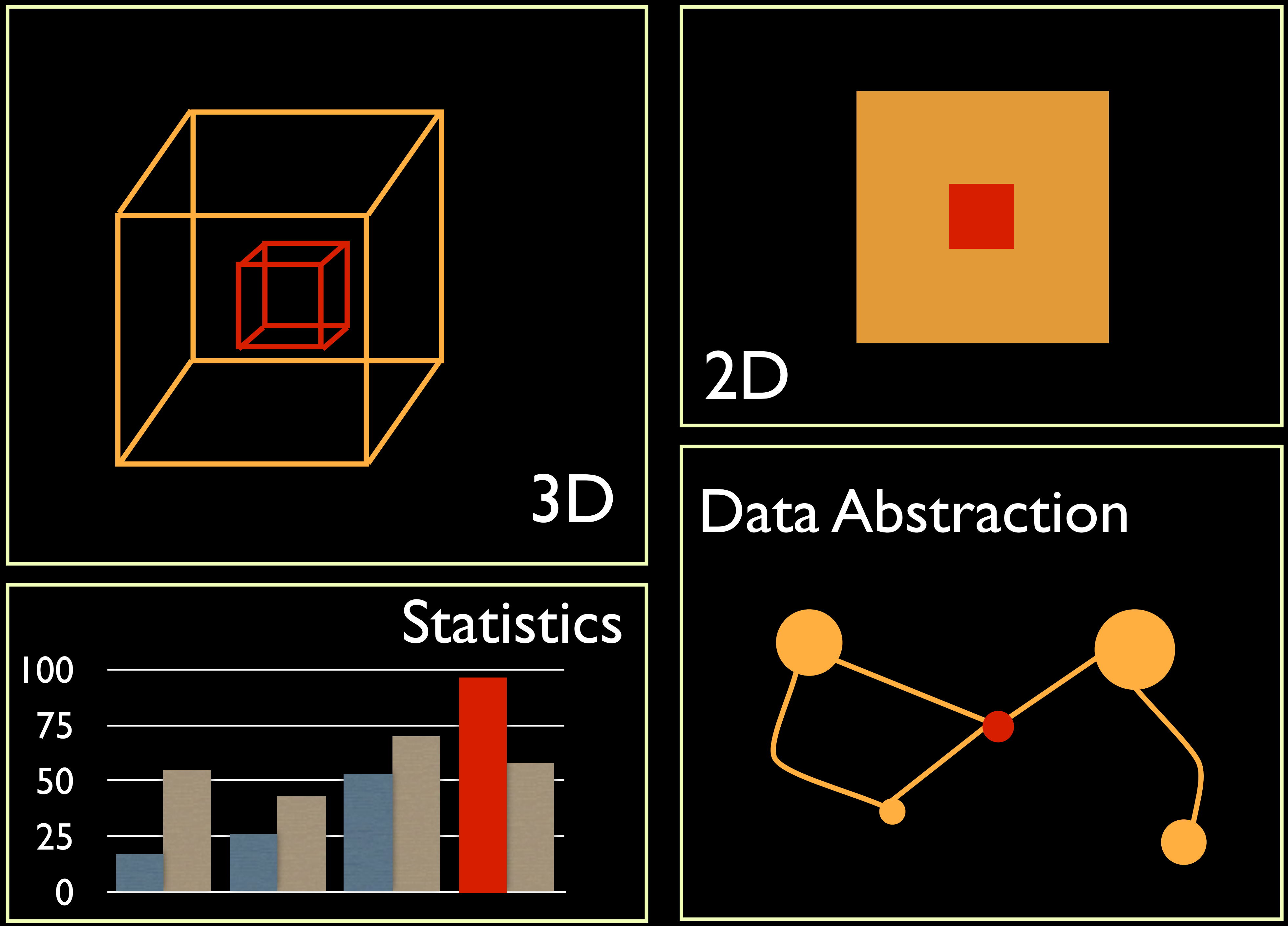

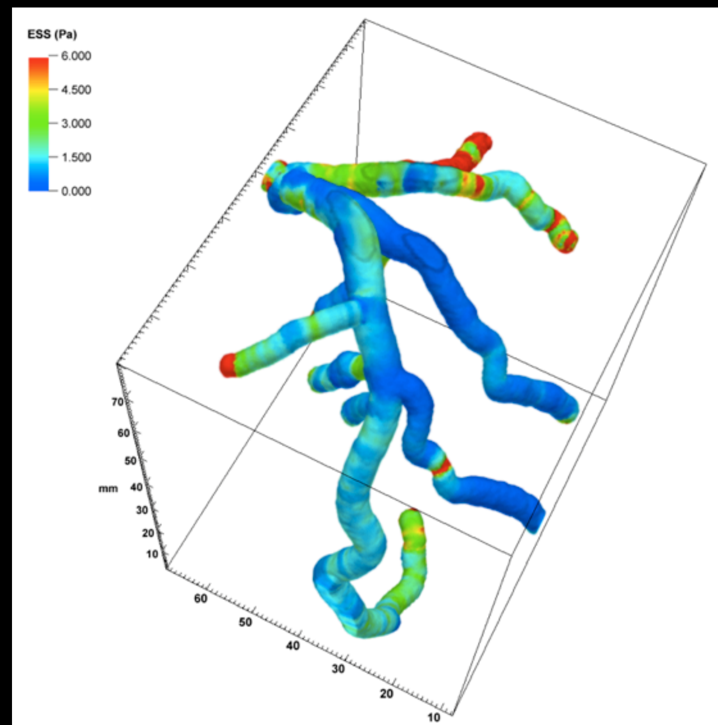

3D

2D

Data Abstraction

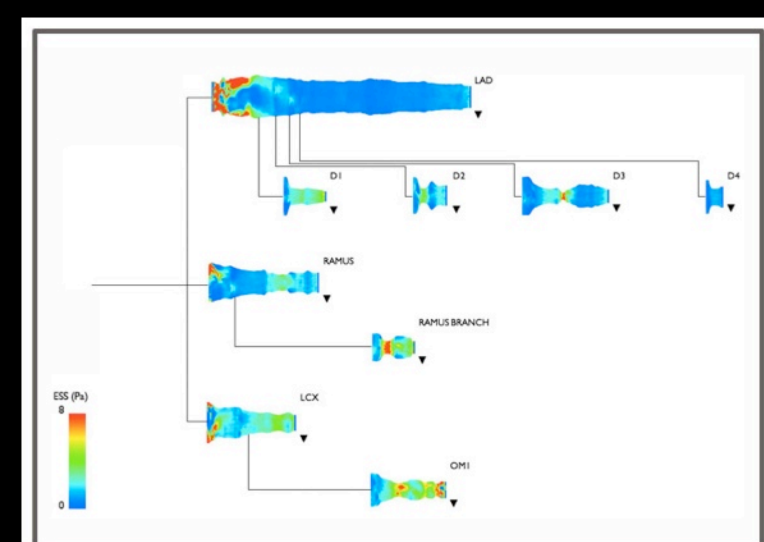

Statistics

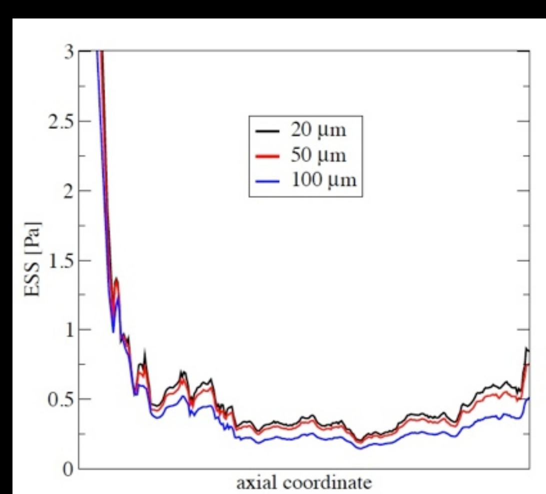

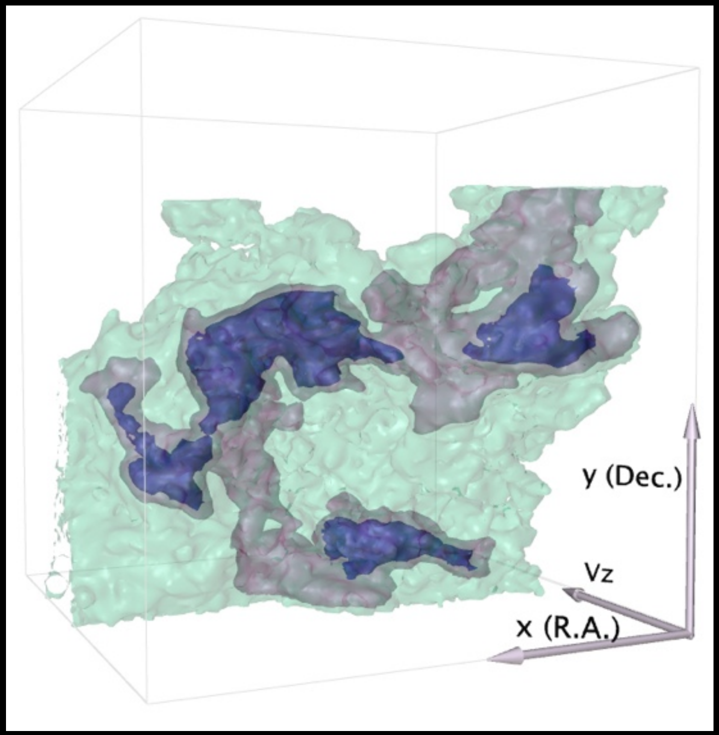

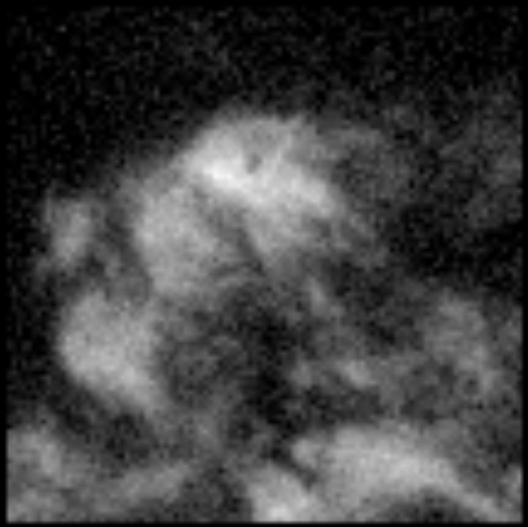

2D

3D

Data Abstraction

Statistics

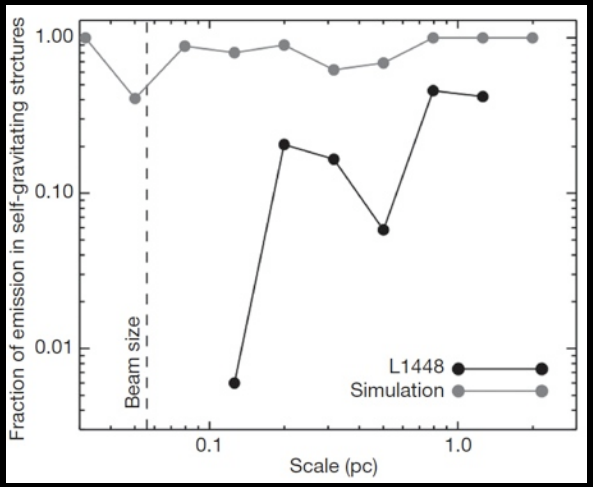

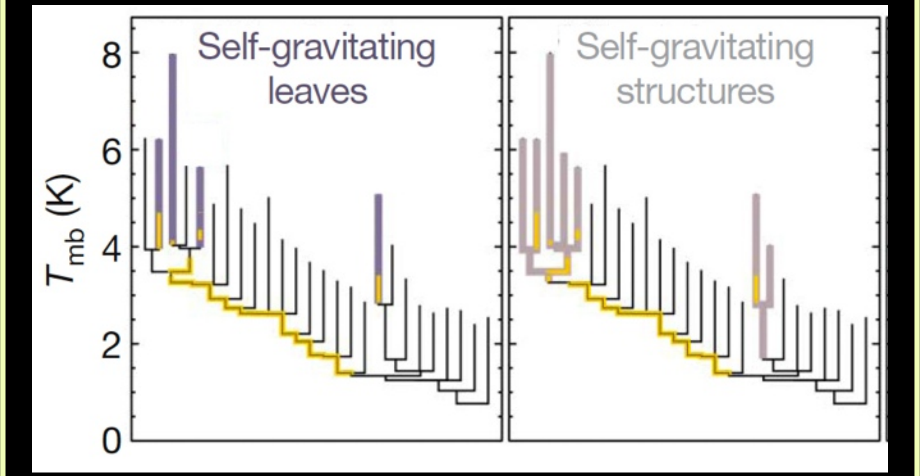

How?

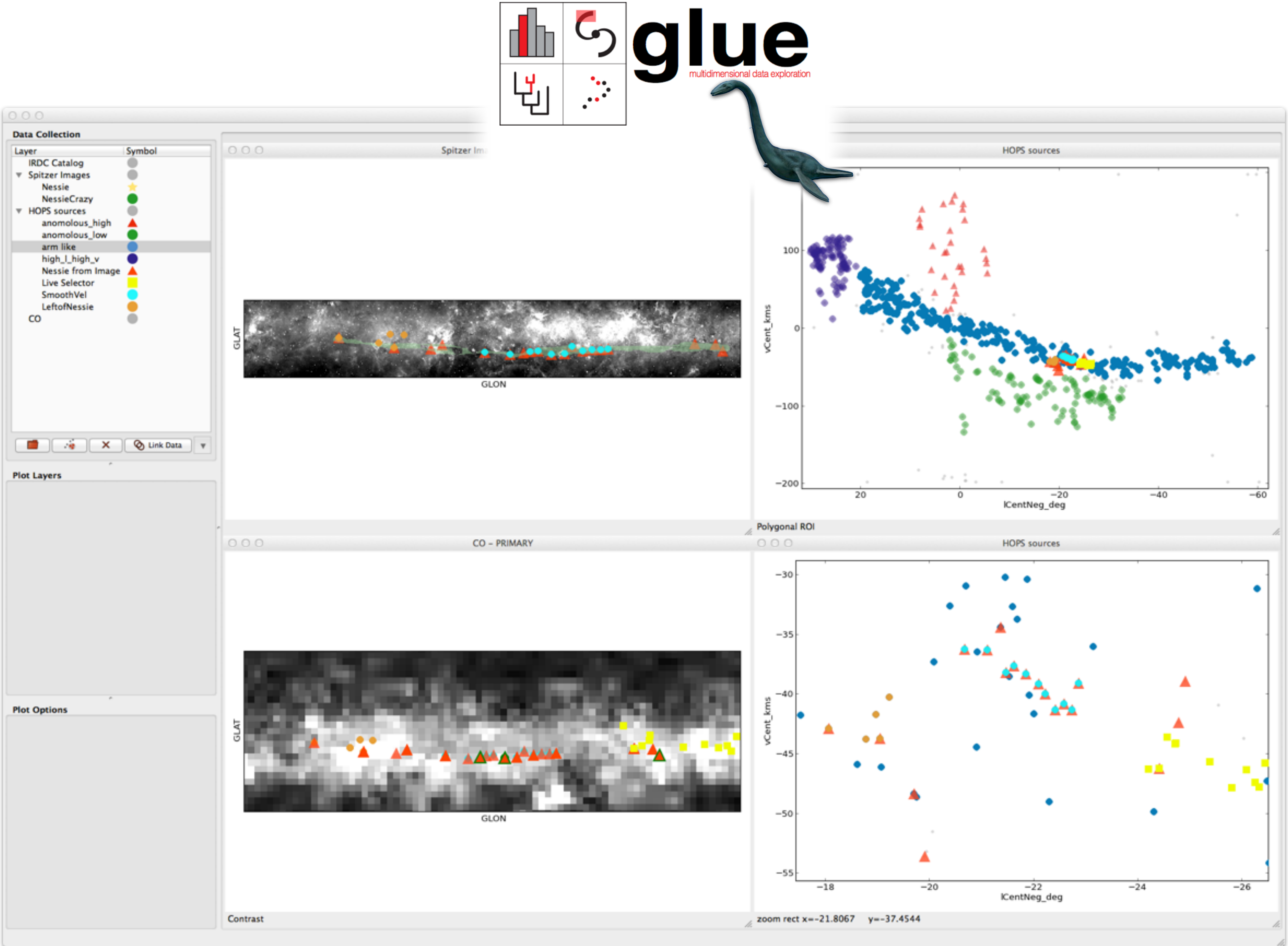

*Glue collaboration: **Beaumont**, Borkin, Goodman, Pfister, Robitaille*

JohnTukey

Astron. Nachr. / AN **333**, No. 5/6, 505 – 514 (2012) / **DOI** 10.1002/asna.201211705

Principles of high-dimensional data visualization in astronomy

A.A. Goodman*

Harvard-Smithsonian Center for Astrophysics, Cambridge, MA, USA

Received 2012 May 3, accepted 2012 May 4
Published online 2012 Jun 15

Key words cosmology: large-scale structure – ISM: clouds – methods: data analysis – techniques: image processing – techniques: radial velocities

Astronomical researchers often think of analysis and visualization as separate tasks. In the case of high-dimensional data sets, though, interactive *exploratory data visualization* can give far more insight than an approach where data processing and statistical analysis are followed, rather than accompanied, by visualization. This paper attempts to charts a course toward "linked view" systems, where multiple views of high-dimensional data sets update live as a researcher selects, highlights, or otherwise manipulates, one of several open views. For example, imagine a researcher looking at a 3D volume visualization of simulated or observed data, and simultaneously viewing statistical displays of the data set's properties (such as an x-y plot of temperature vs. velocity, or a histogram of vorticities). Then, imagine that when the researcher selects an interesting group of points in any one of these displays, that the same points become a highlighted subset in all other open displays. Selections can be graphical or algorithmic, and they can be combined, and saved. For tabular (ASCII) data, this kind of analysis has long been possible, even though it has been under-used in astronomy. The bigger issue for astronomy and other "high-dimensional" fields, though, is that no extant system allows for full integration of images and data cubes within a linked-view environment. The paper concludes its history and analysis of the present situation with suggestions that look toward cooperatively-developed open-source modular software as a way to create an evolving, flexible, high-dimensional, linked-view visualization environment useful in astrophysical research.

The Bones of the Milky Way

Alyssa A. Goodman (Harvard-Smithsonian Center for Astrophysics)

with collaborators at (alphabetically by insitution):

Boston University: James Jackson

Caltech: Jens Kauffmann

Harvard - Smithsonian: Christopher Beaumont, Michelle A. Borkin, Thomas M. Dame

Max Planck Insitute for Astronomy: Thomas Robitaille

U. Munich: Andreas Burkert

U. Vienna: Joao F. Alves

U. Wisconsin: Robert A. Benjamin

Authorea

ALYSSA GOODMAN

Article view

Folder view

Newsfeed view

Article index

Abstract

Co author instructions

Introduction 1

Nessie longer

1nessie findingchart

Table1 mass nessie

3d position

2galactic coords

Using rotation curves

6drafttopview

3draftnessie vrad 21

Co velocities

4draft co sky

Nh3 velocities

5draft side view

7draftnessie co lv

Significance

Bones dobbs

Quick edit

How do I..?

OPEN SCIENCE ARTICLE

WORKING DRAFT

Last updated 5 days ago by Joao Alves

The Bones of the Milky Way

Alyssa Goodman, Joao Alves, Chris Beaumont, Tom Dame, James Jackson, Jens Kauffmann, Thomas Robitaille, Alberto Pepe, Michelle Borkin, Andreas Burkert, Bob Benjamin

+ Add author

Export article

Abstract. The very long, thin infared dark cloud ``Nessie" is even longer than had been previously claimed, and an analysis of its Galactic location suggests that it lies directly in the Milky Way's mid-plane, tracing out a highly elongated bone-like feature within the prominent Scutum-Centaurus spiral arm. Re-analysis of mid-infrared imagery from the Spitzer Space Telescope shows that this IRDC is at least 2, and possibly as many as 8 times longer than had originally been claimed by Nessie's discoverers, Jackson et al. (2001); its aspect ratio is therefore at least 150:1, and possibly as large as 800:1. A careful accounting for both the Sun's offset from the Galactic plane (~ 25 pc) and the Galactic center's offset from the $(l^{II}, b^{II}) = (0,0)$ position defined by the IAU in 1959 shows that the latitude of the true Galactic mid-plane at the 3.1 kpc distance to the Scutum-Centaurus Arm is not $b = 0$, but instead closer to $b = -0.5$, which is the latitude of Nessie to within a few pc. Apparently, Nessie lies *in* the Galactic mid-plane. An analysis of the radial velocities of low-density (CO) and high-density (NH_3) gas associated with the Nessie dust feature suggests that Nessie runs along the Scutum-Centaurus Arm in position-position-velocity space, which means it likely forms a dense 'spine' of the arm in real space as well. No galaxy-scale simulation to date has the spatial resolution to predict a Nessie-like feature, but extant simulations do suggest that highly elongated over-dense filaments should be associated with a galaxy's spiral arms. Nessie is situated in the closest major spiral arm to the Sun toward the inner Galaxy, and appears almost perpendicular to our line of sight, making it the easiest feature of its kind to detect from our location (a shadow of an Arm's bone, illuminated by the Galaxy beyond). Although the Sun's offset from the Galactic plane is not significant compared with the thickness of the plane as traced by Population I objects such as GMCs and HII regions, it may be significant compared with an extremely thin layer that might be traced out by Nessie-like objects. Future high-resolution extinction and molecular line data may therefore allow us to exploit the Sun's position above the plane to gain a small amount of perspective on the Galactic disk.

Alyssa Goodman, m:617-230-7080; url: milkywaybones.org

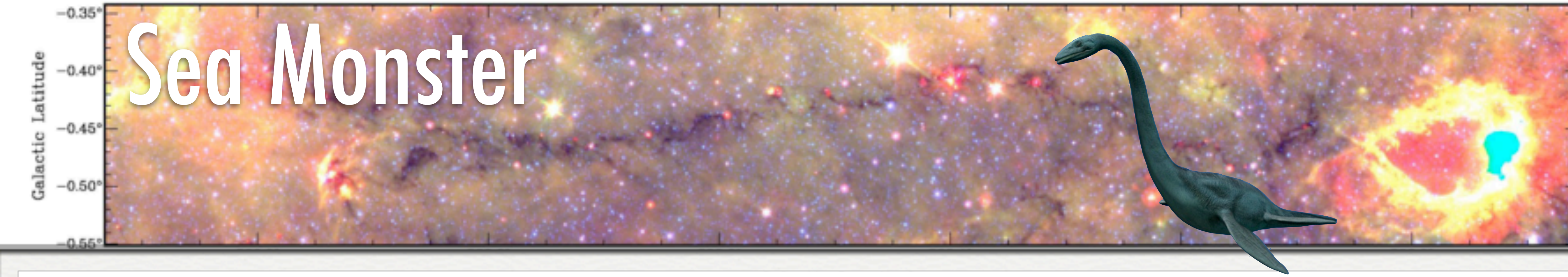

The Astrophysical Journal Letters, 719:L185–L189, 2010 August 20 doi:10.1088/2041-8205/719/2/L185

THE “NESSIE” NEBULA: CLUSTER FORMATION IN A FILAMENTARY INFRARED DARK CLOUD

James M. Jackson[1], Susanna C. Finn[1], Edward T. Chambers[2], Jill M. Rathborne[3], and Robert Simon[4]
[1] Institute for Astrophysical Research, Boston University, Boston, MA 02215, USA; jackson@bu.edu, sfinn@bu.edu
[2] Department of Physics and Astronomy, Northwestern University, Evanston, IL 60208, USA; e-chambers@northwestern.edu
[3] Australia Telescope National Facility and Universidad de Chile, Santiago, Chile; rathborn@das.uchile.cl
[4] I. Physikalisches Institut, Universität zu Köln, 50937 Köln, Germany; simonr@ph1.uni-koeln.de
Received 2010 April 13; accepted 2010 July 21; published 2010 August 3

ABSTRACT

The “Nessie” Nebula is a filamentary infrared dark cloud (IRDC) with a large aspect ratio of over 150:1 ($1\overset{\circ}{.}5 \times 0\overset{\circ}{.}01$ or 80 pc × 0.5 pc at a kinematic distance of 3.1 kpc). Maps of HNC (1–0) emission, a tracer of dense molecular gas, made with the Australia Telescope National Facility Mopra telescope, show an excellent morphological match to the mid-IR extinction. Moreover, because the molecular line emission from the entire nebula has the same radial velocity to within ± 3.4 km s^{-1}, the nebula is a single, coherent cloud and not the chance alignment of multiple unrelated clouds along the line of sight. The Nessie Nebula contains a number of compact, dense molecular cores which have a characteristic projected spacing of ∼4.5 pc along the filament. The theory of gravitationally bound gaseous cylinders predicts the existence of such cores, which, due to the “sausage” or “varicose” fluid instability, fragment from the cylinder at a characteristic length scale. If turbulent pressure dominates over thermal pressure in Nessie, then the observed core spacing matches theoretical predictions. We speculate that the formation of high-mass stars and massive star clusters arises from the fragmentation of filamentary IRDCs caused by the “sausage” fluid instability that leads to the formation of massive, dense molecular cores. The filamentary molecular gas clouds often found near high-mass star-forming regions (e.g., Orion, NGC 6334, etc.) may represent a later stage of IRDC evolution.

Key words: ISM: clouds – stars: formation

Jackson et al. 2010

Wednesday, February 6, 2013

Monster to Bone

There could be ~1000 more of these to find...a full skeleton perhaps?

milkywaybones.org

Ringberg Castle, Bavaria
"Early Phases of Star Formation"
July 2012

Question *Andi Burkert*: Is Nessie "parallel to the Galactic Plane"?

Answer *no one* immediately knew the answer!

AG decides to look into this and...

“Is Nessie Parallel to the Galactic Plane?”

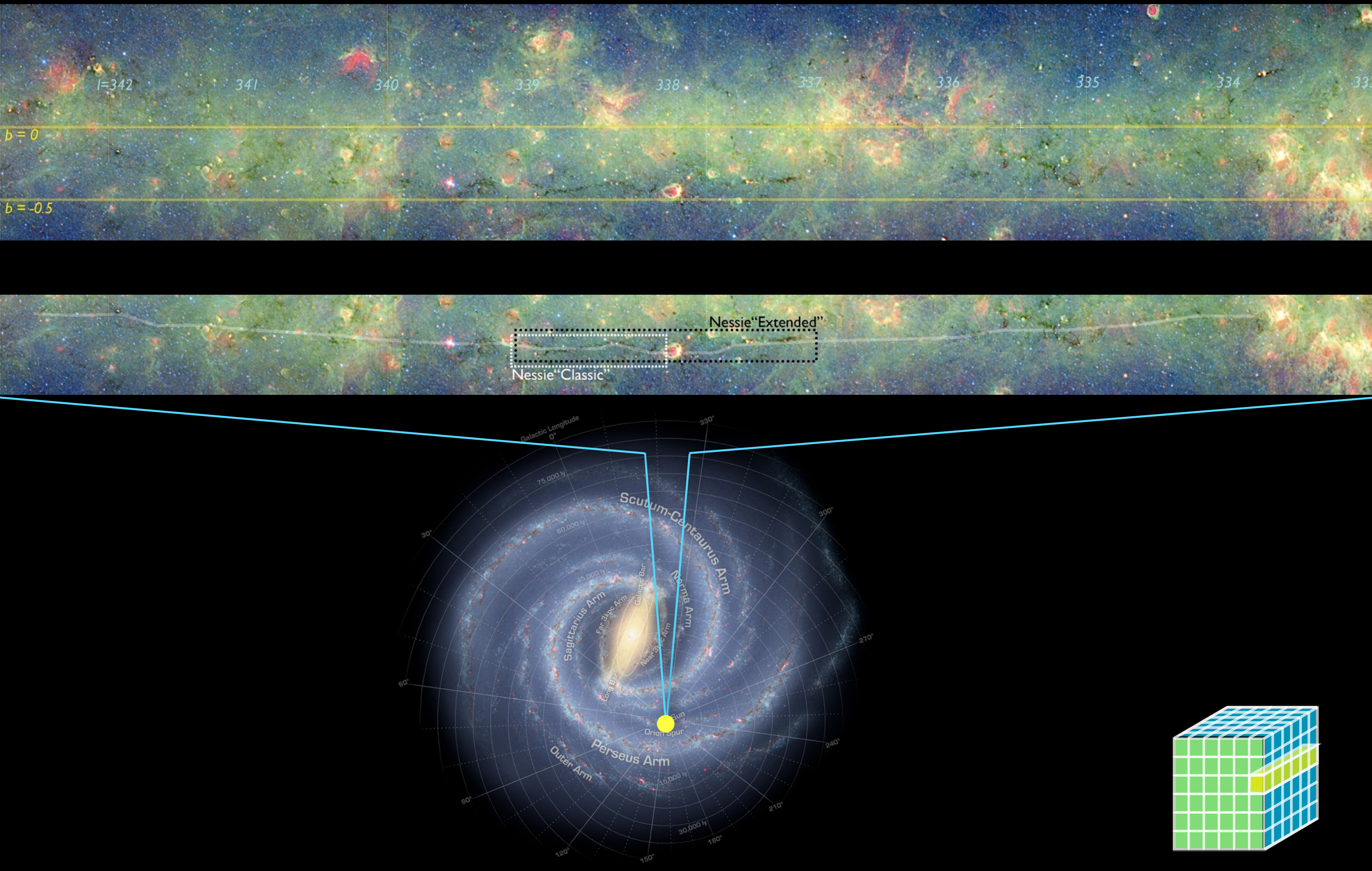
l=342
341
340
339
338
337
336
335
334
333
b = 0
b = -0.5
Nessie"Extended"
Nessie"Classic"
Galactic Longitude
0°
330°
300°
270°
240°
210°
180°
150°
120°
90°
60°
30°
75,000 ly
60,000 ly
45,000 ly
30,000 ly
15,000 ly
Scutum-Centaurus Arm
Norma Arm
Galactic Bar
Far 3kpc Arm
Near 3kpc Arm
Sagittarius Arm
Long Bar
Sun
Orion Spur
Perseus Arm
Outer Arm

The Milky Way

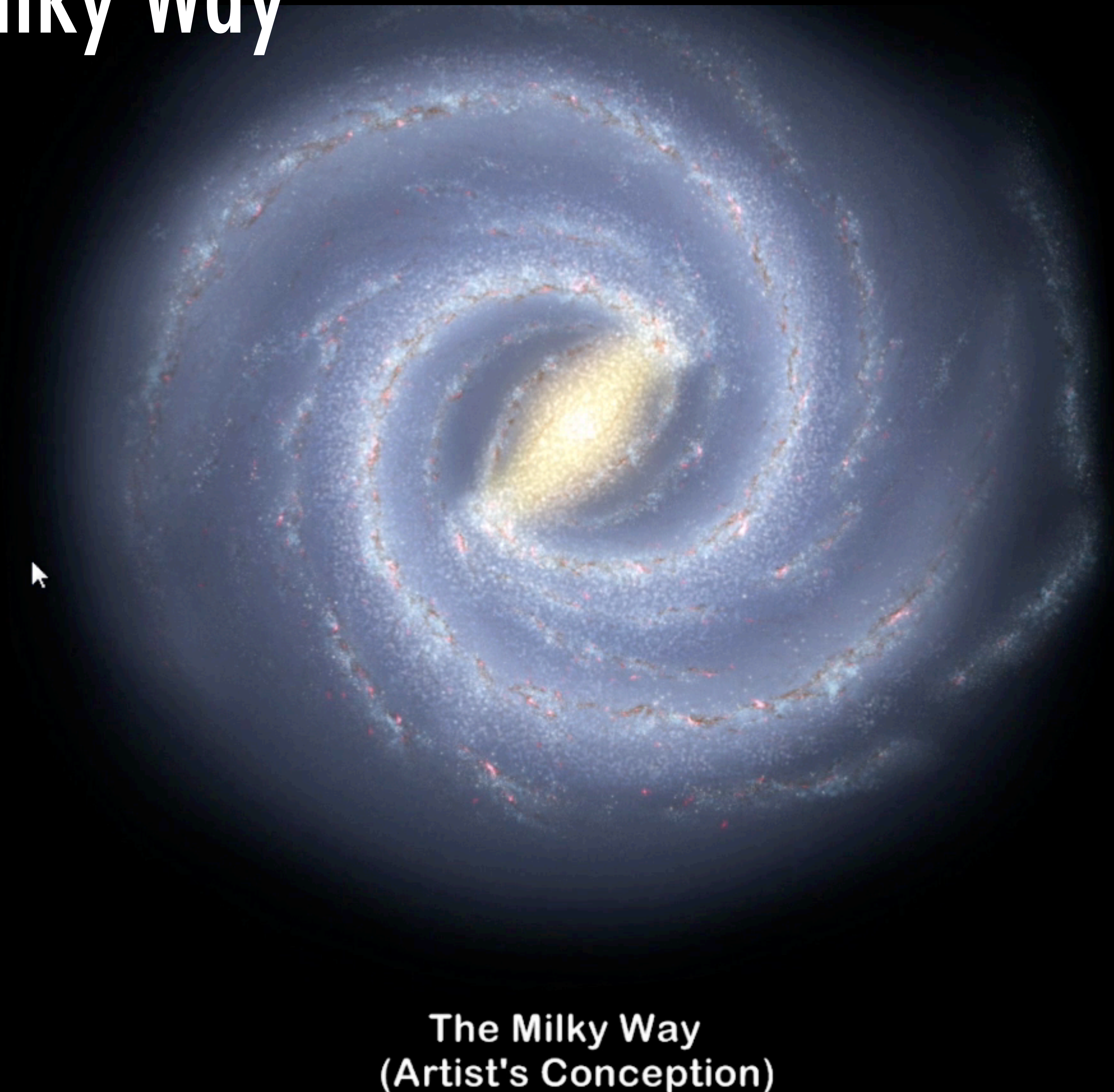

Using Velocity Constraints

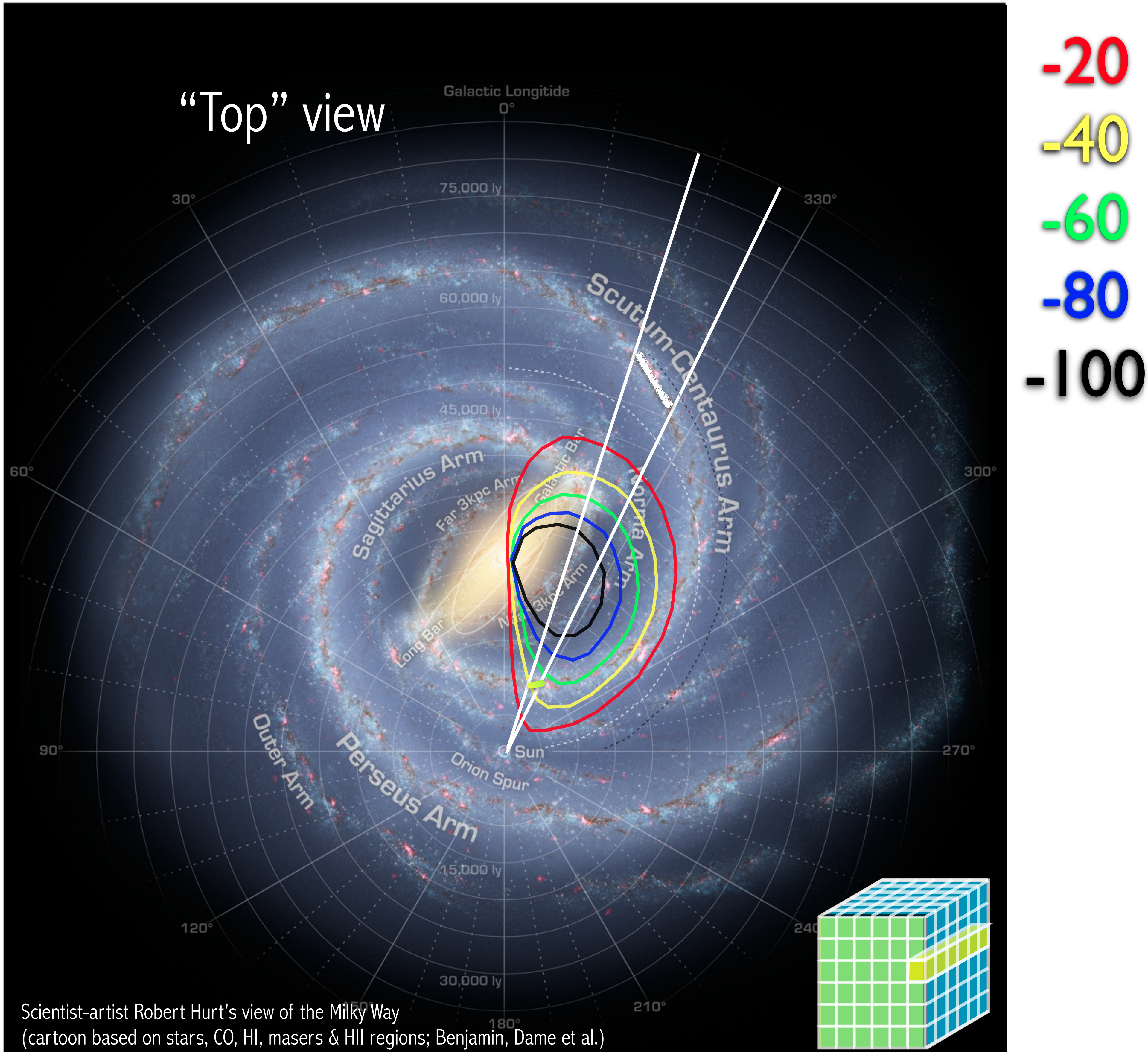

Scientist-artist Robert Hurt's view of the Milky Way
(cartoon based on stars, CO, HI, masers & HII regions; Benjamin, Dame et al.)

Using Velocity Constraints

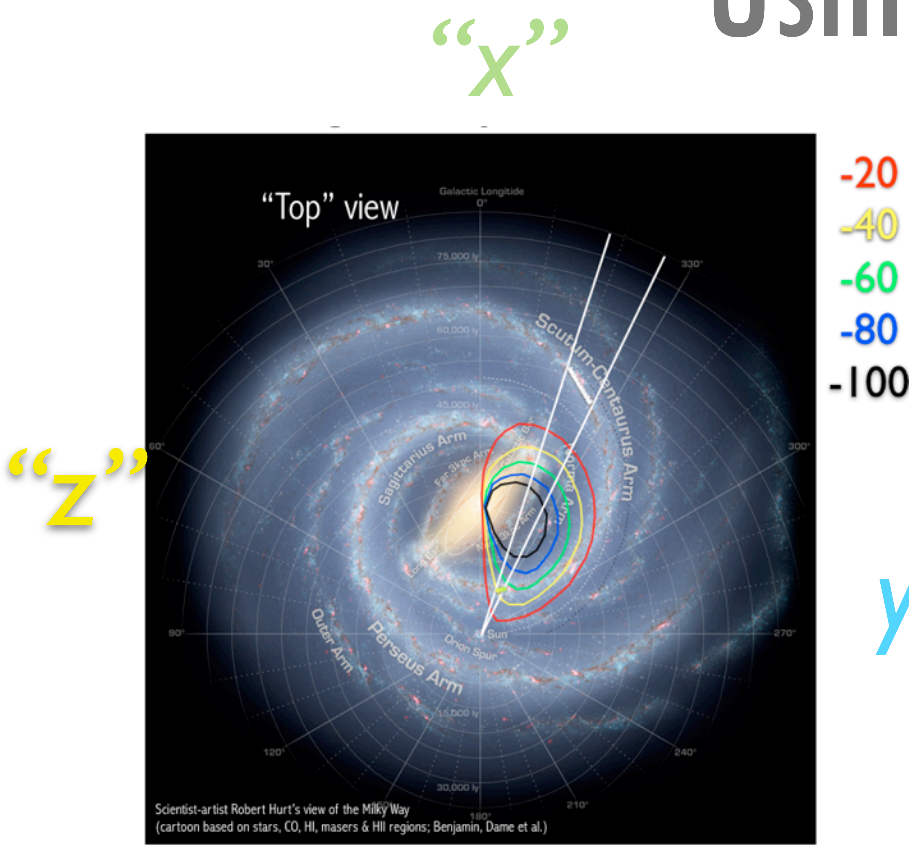

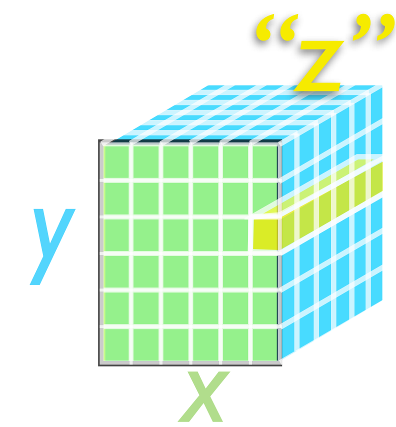

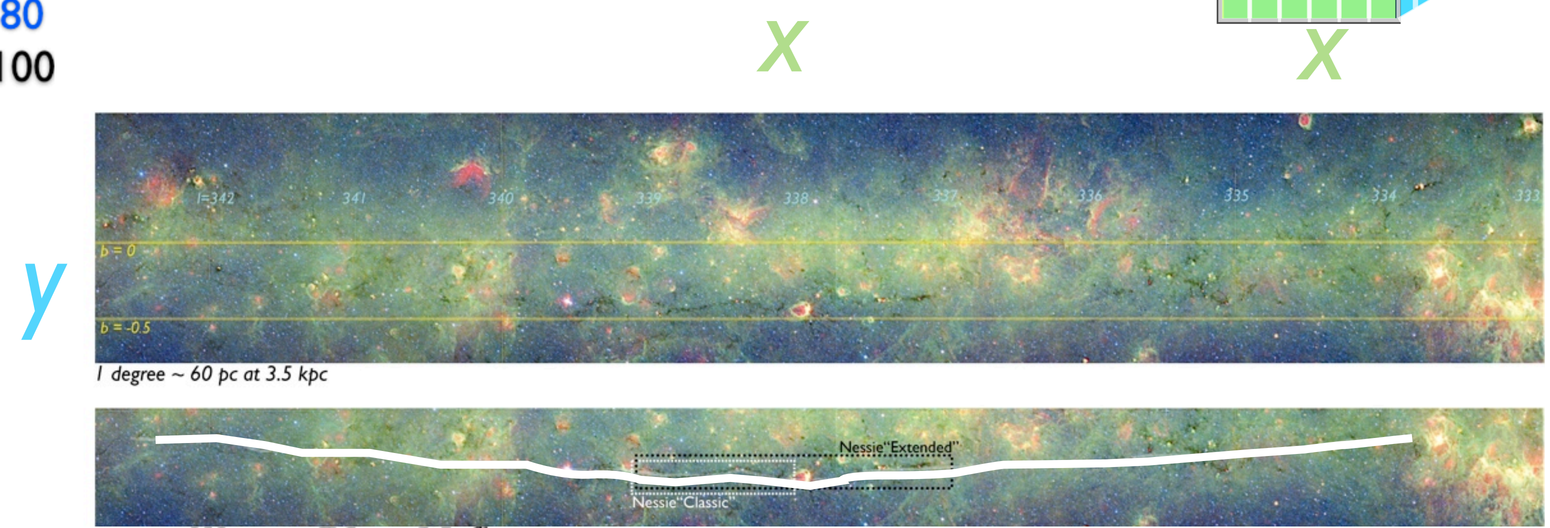

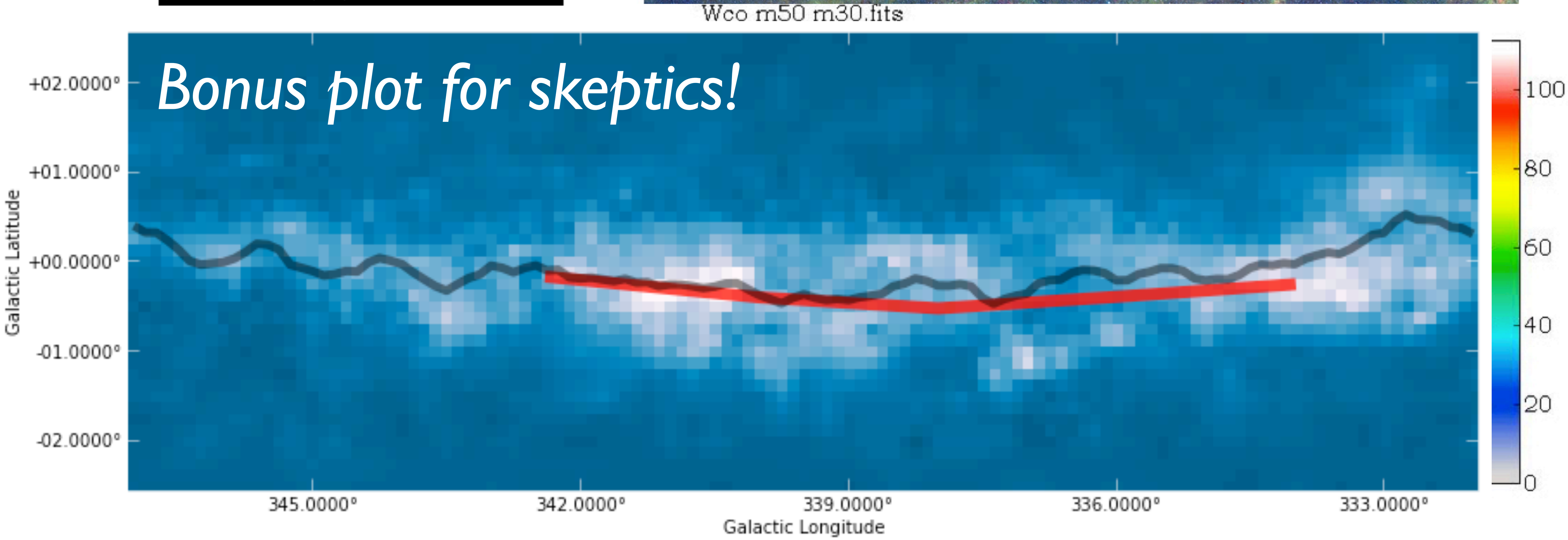

Why b<0?!
Galactic Geometry: 1959 and Now

Drawing is schematic--NOT to scale

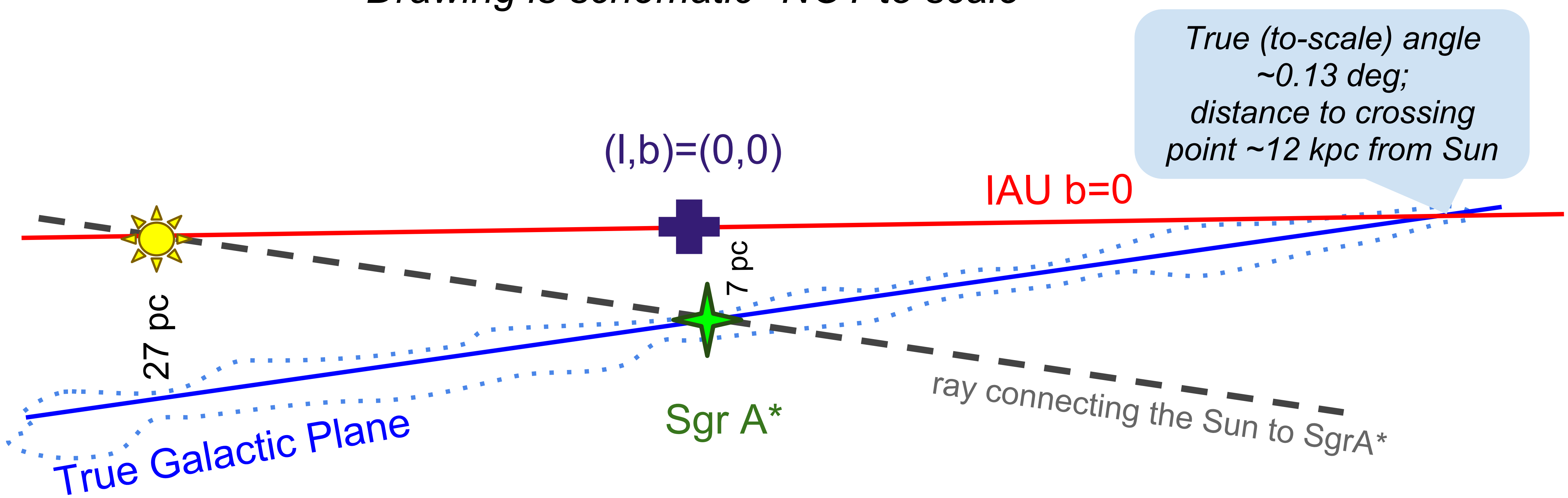

The equatorial plane of the new co-ordinate system must of necessity pass through the sun. It is a fortunate circumstance that, within the observational uncertainty, both the sun and Sagittarius A lie in the mean plane of the Galaxy as determined from the hydrogen observations. If the sun had not been so placed, points in the mean plane would not lie on the galactic equator. *[Blaauw et al. 1959]*

Predicted Near & Far Scutum-Centaurus Arm

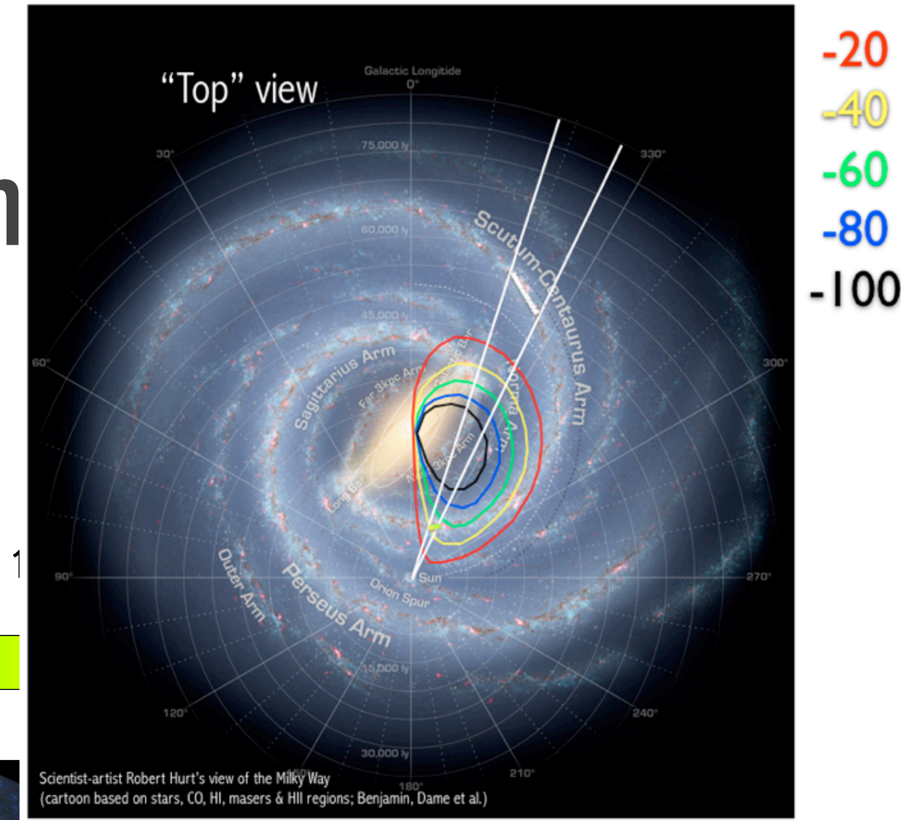

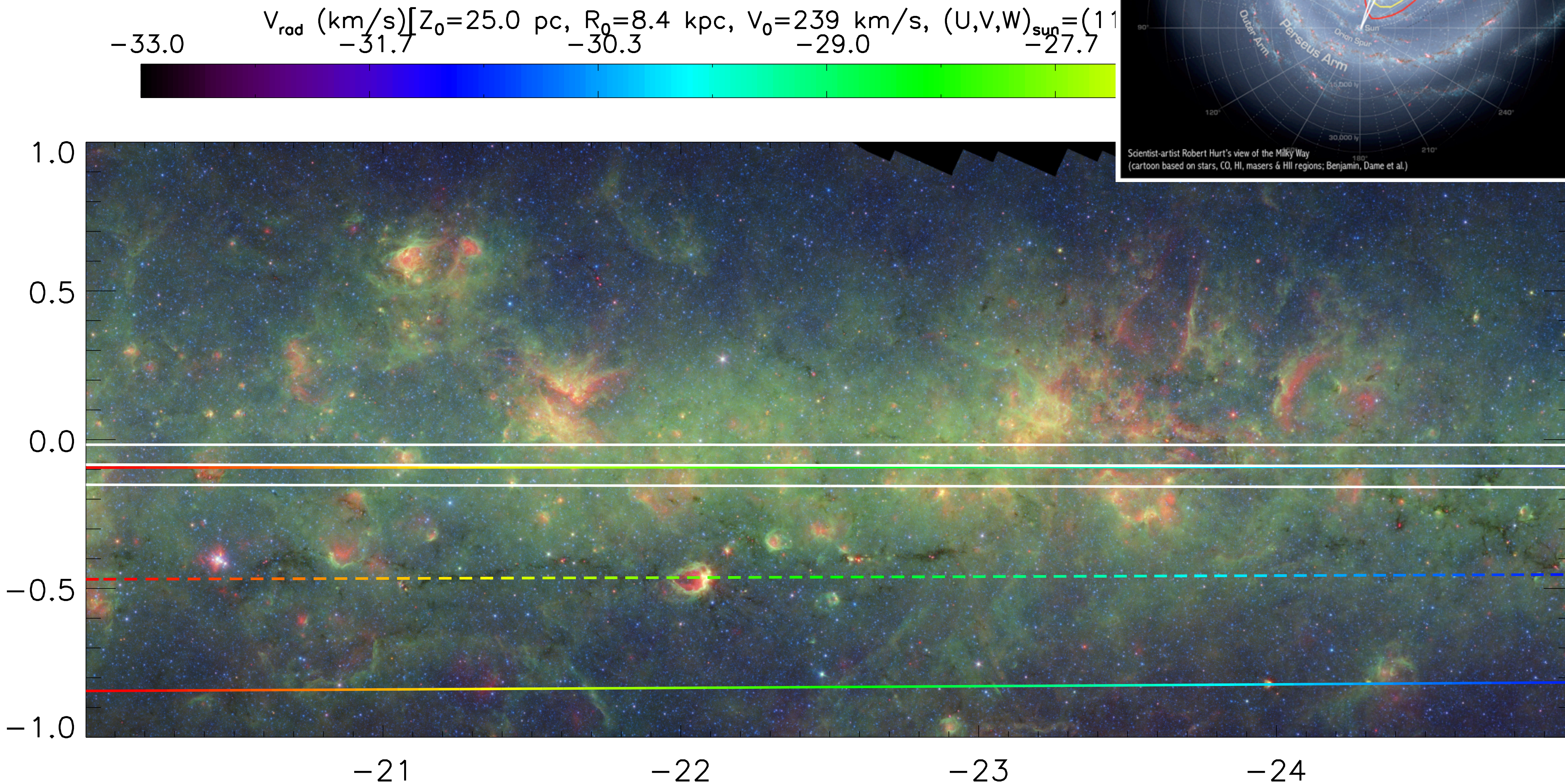

Predicted Velocities match NH_3 Cores in Nessie Perfectly

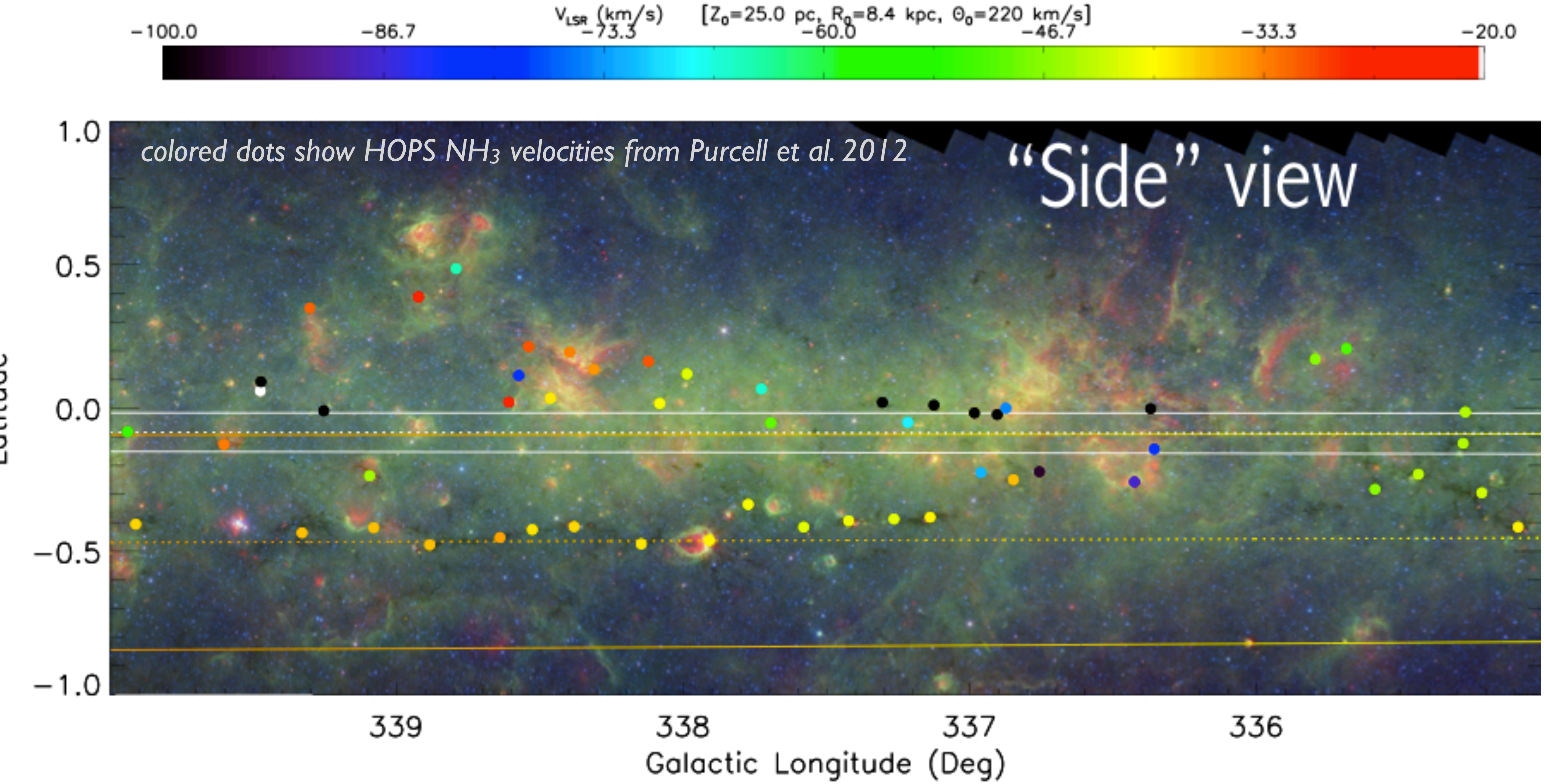

Predicted Velocities match NH_3 Cores in Nessie Perfectly

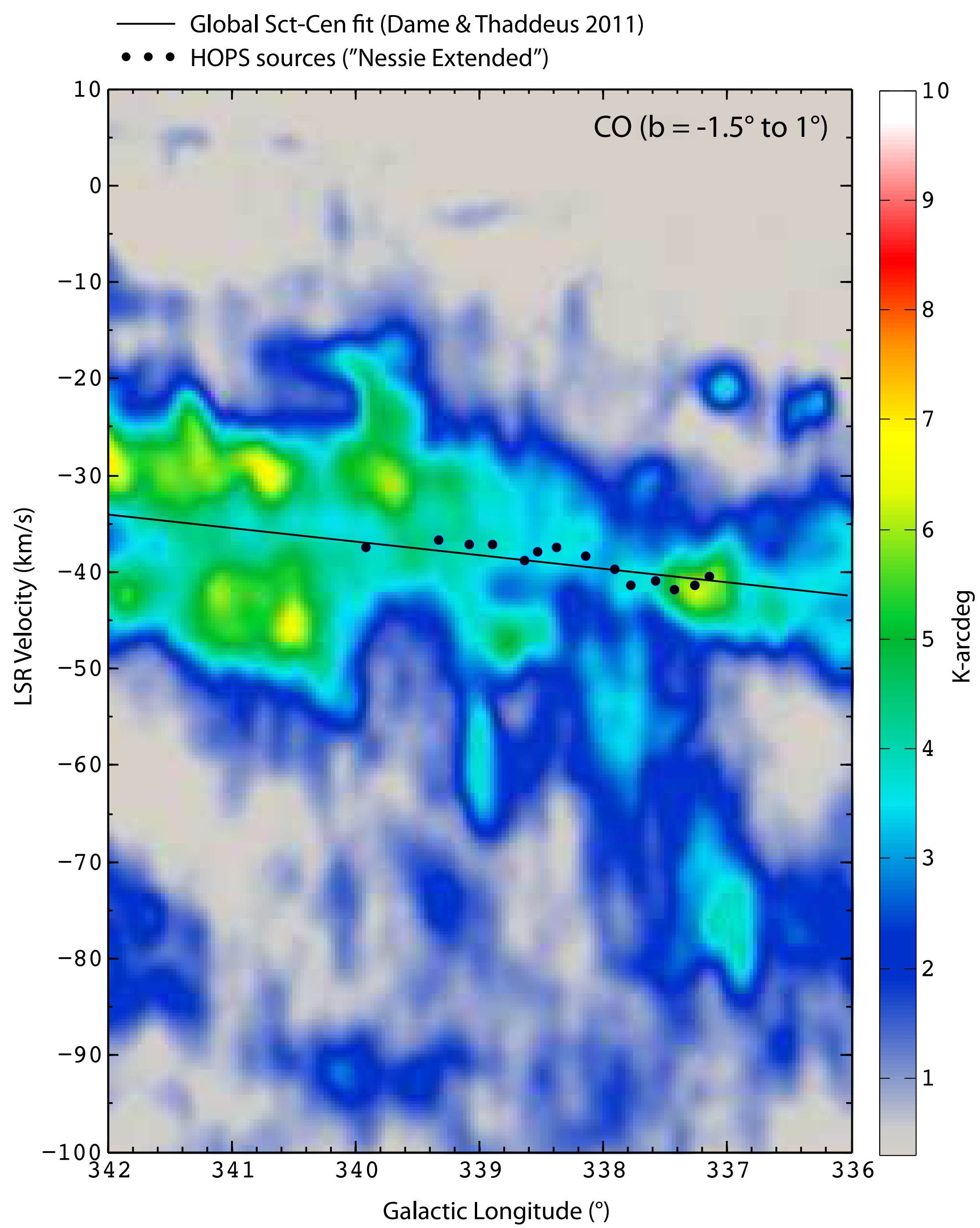

black dots show HOPS NH_3 velocities from Purcell et al. 2012; color is CO; line is log-spiral fit to full Scut-Cen Arm

Nessie is a Bone of the Milky Way

(flipped) image of IC342 from Jarrett et al. 2012; WISE Enhanced Resolution Galaxy Atlas

What does that mean?

(flipped) image of IC342 from Jarrett et al. 2012; WISE Enhanced Resolution Galaxy Atlas

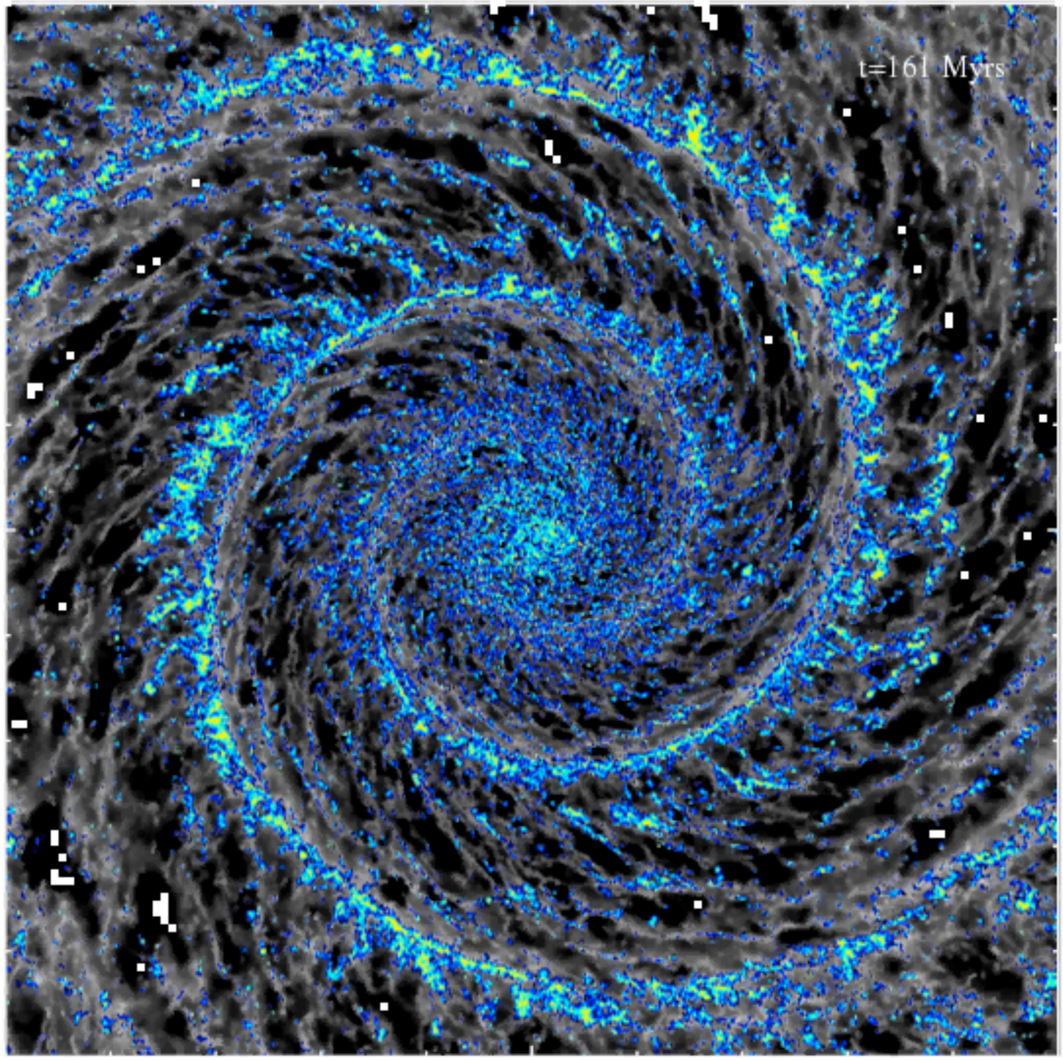

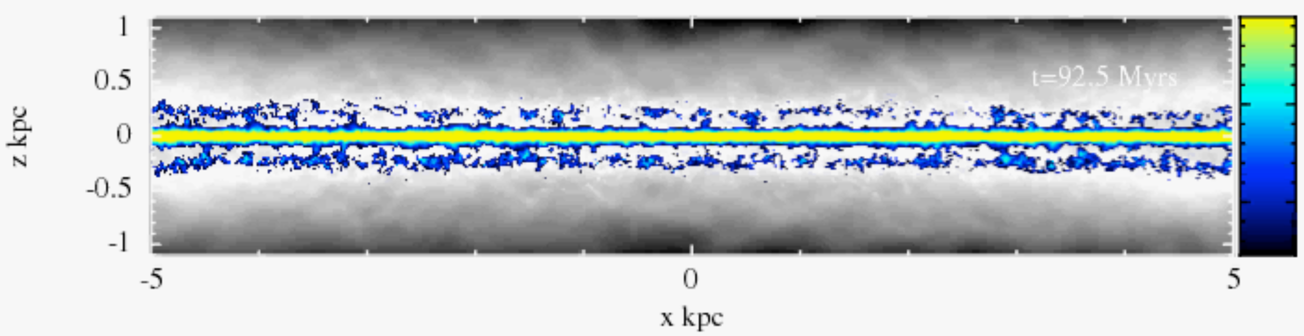

simulations courtesy Clare Dobbs

"Diskovering" the Milky Way

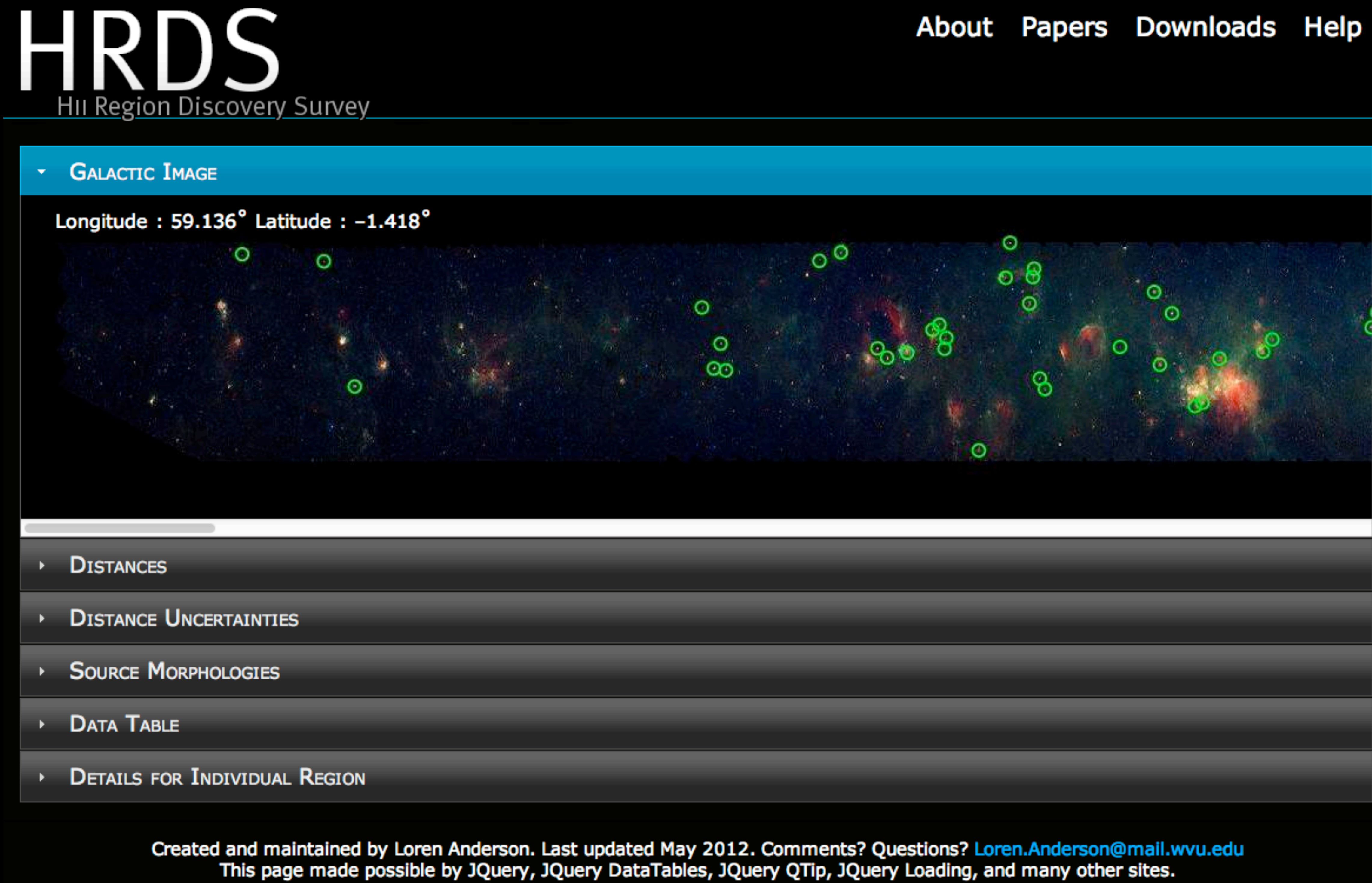

Loren Anderson (West Virginia University), Thomas Bania (Boston U.), Dana Balser (NRAO), Bob Rood (U. Virginia), and Trey Wenger (Boston U.)

The Future

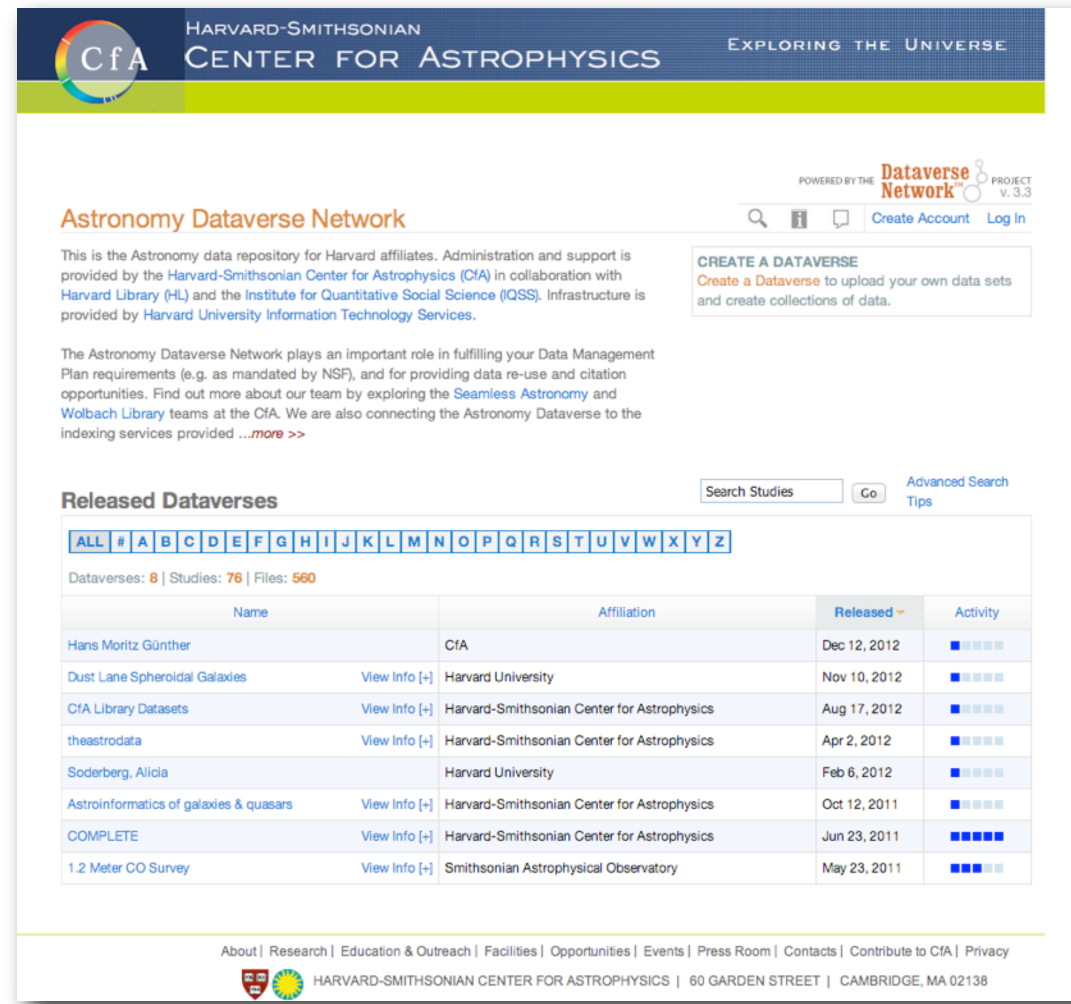

seamless access to tools, data, analysis, discourse

UNIVERSE3D.org

The Bones of the Milky Way: Credits

Seamless Astronomy-style tools used in this project

SEAMLESS ASTRONOMY
Linking scientific data, publications, and communities

- authorea.com (open publishing)
- theastrodata.org (open data)
- glueviz.org (open source tools)
- universe3d.org (collaborative data)
- worldwidetelescope.org (universe information system)
- virtual observatory standards (international online information-sharing systems)

Supported by

Microsoft Research · NSF · NASA · VE RI TAS · Smithsonian

Alyssa Goodman, m:617-230-7080; milkywaybones.org

Microsoft® Research
WorldWide Telescope

Experience WWT at **worldwidetelescope.org**

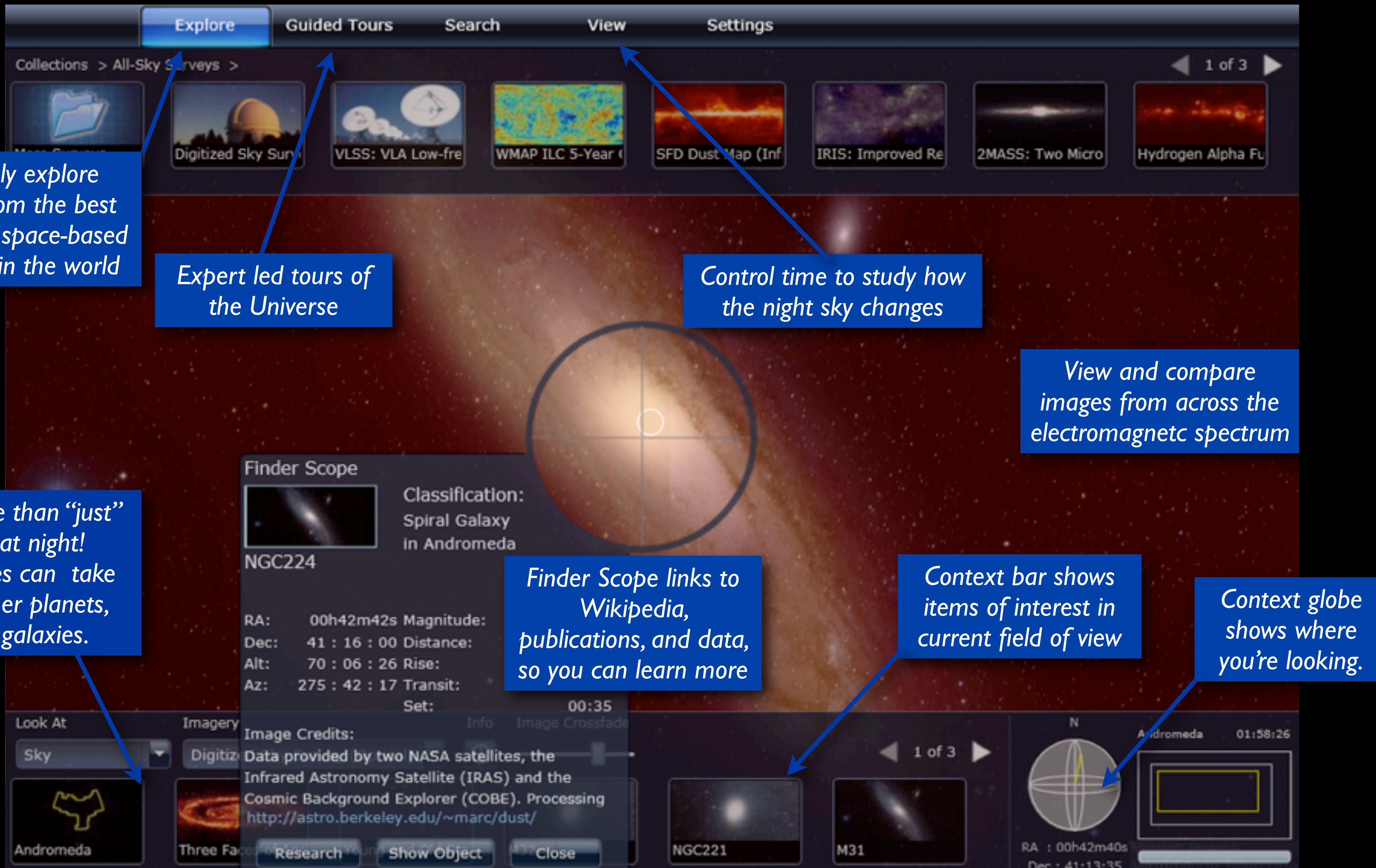

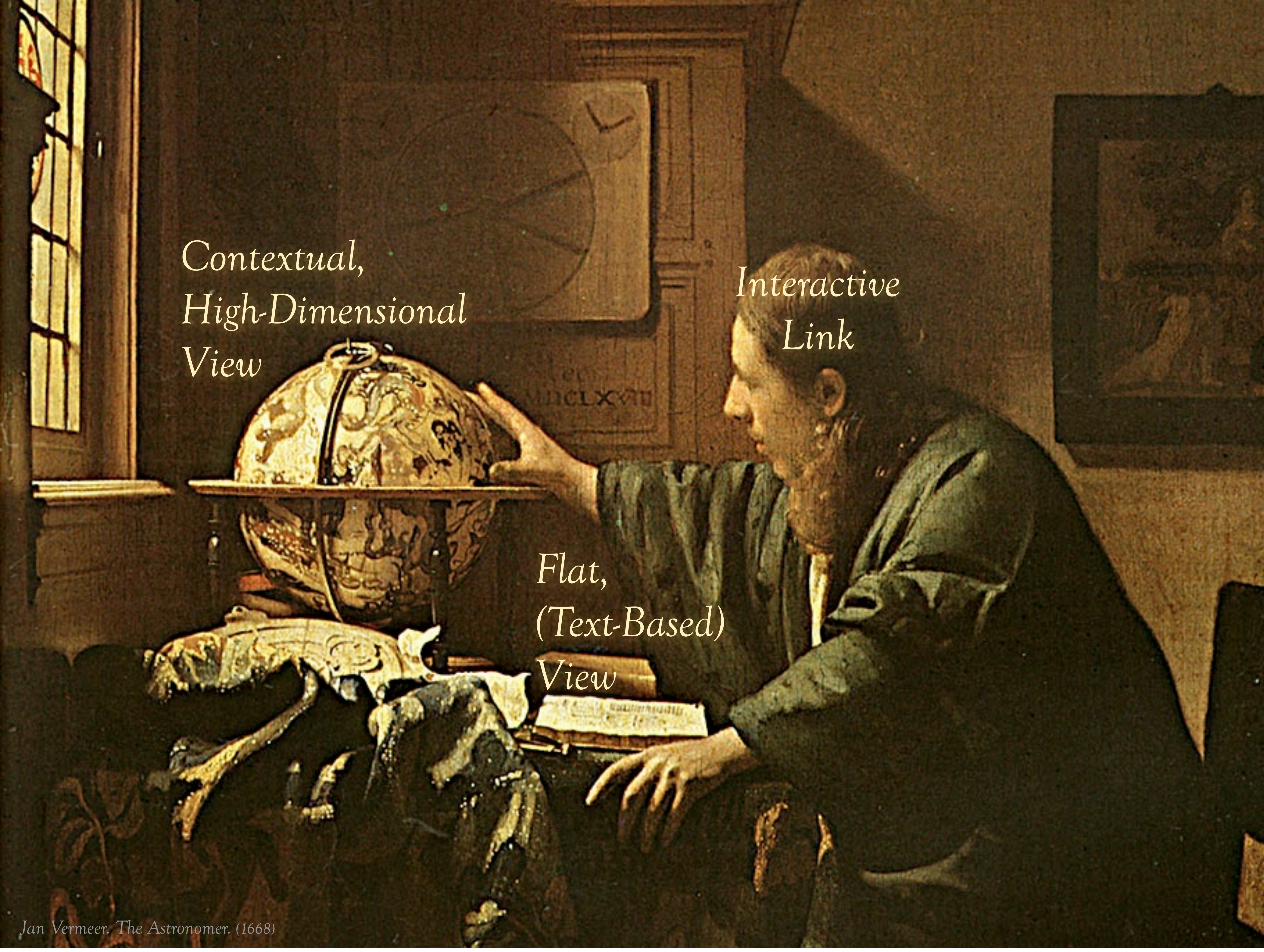
Contextual,
High-Dimensional
View
Interactive
Link
Flat,
(Text-Based)
View
Jan Vermeer. The Astronomer. (1668)